الجمهورية الجزائرية الديمقراطية الشعبية
People's Democratic Republic of Algeria
وزارة التعليم العالي والبحث العلمي
Ministry of Higher Education and Scientific Research
جامعة سعد دحلب البليدة
Saad dahlab University
كلية التكنولوجيا
Faculty of technology
قسم الإلكترونيك
Electronics departement

Master Thesis

Microelectronic specialty

Presentedby

Aissaoui Youcef &Boulahchiche Rafik

Study of multiple quantum dots structures based on InGaN/GaN semiconductor for photovoltaic cell

Proposed by :PrA.Aissat

University year 2019-2020

Acknowledgement

This work was carried out at the laboratory (LATSI) Department of Electronics Faculty of Science of the engineer Saad Dahlab University of Blida.

First of all , thanks and praise to **ALLAH** Almighty for granting me the will, courage, and patience to complete this work.

I would like to thank P r**Aissat Abdelkader**for having supervised this work withcompetence and availability.

I would like to express my sincere gratitude and my warm thanks to**Mr. GuessmiHocine**whoparticipated in the evolution of my work and its manufacture.

I would like to thank **Mr**.**LaidouciAbdelmoumen**for his help and wise advice.

I thank the members of the jury for agreeing to judge this work.

My feelings of deep gratitude go to my teachers who throughout the years of study have passed on their knowledge to us without reservation.

I also thank my friends for their help and all the people who have helped me from near or far to carry out this work.

Dedication

We dedicate our dissertation work to our families and. A special feeling of gratitude to Our loving parents, whose words of encouragement and push for tenacity ring in our ears. We also dedicate this dissertation to our many friends who have supported us throughout the process. We will always appreciate all they have done,

We dedicate this work and give special thanks to Z.Maamar , A.Ayache . A.Djamel.

ملخص :

في هذا العمل، صببنا اهتمامنا على دراسة ومحاكاة ونمذجة خلايا شمسية بنقاط كموميةأساسها(InGaN/GaN)هذا الخليط الثلاثي الذي هو من أشباه النواقل ،III-Vيمثّل خصائص جد مهمة وخاصة طاقة فجوته التي هي على شكلمباشر.

لقد قمنا أيضا بدراسة مختلف العناصر التي تميز الخلية الضوئية، وقد تحقق أداء الخلايا الشمسية لبنيات مختلفة بفضلبرنامج Silvaco TCADتمت مقارنة النتائج التي تم الحصول عليها لتحديد أفضل بنية.

كلمات المفاتيح :نقاط كم، تطبيق ضوئي، أنصاف النواقل، طاقة الفجوة

Résumé : Dans ce travail, nous nous sommes intéressés à l'étude, la simulation et lamodélisation des cellules solaires à boîtes quantiques à base de (InGaN/GaN). Cet alliageternaire qui est un semi-conducteur III-V présente des caractéristiques importantesnotamment son énergie de gap qui est sous forme directe.Nous avons également étudié les différents paramètres caractérisant la cellule solairedont Les performances pour différentes structures ont été réalisées grâce au logicielSilvaco TCAD. Les résultats obtenus ont été comparé afin de déterminer la meilleurestructure.

Mots clés : Boîtes quantiques ; Cellule solaire ; Semi-conducteur ; Energie de gap

Abstract:

In this work, we were interested about the study, the simulation and themodelingof(InGaN/GaN) quantum dots solar cells. This ternary alloy who is an III-V semiconductor present an important characteristic especially its band-gap energy which is in a direct form. We had also studied a different parameter characterized the solar cells where the performances were realized thanks to the software Silvaco TCAD. The results obtained were compared to determine the best structure.

Keywords: Quantum dots; Solar cells; Semiconductor; Bandgap energy.

Lists of acronyms and abbreviations

Acronymes	Signification
Eg	Bandgapenergy
Ga	Galium
As	Arsenic
P	Phosphore
FCC	Face-centeredcubic
B_c	Conduction band
B_v	Valence band
λ_b	De Broglie Wavelength
m^*	The effective mass of the electron
λ_{th}	Thermal de Broglie Wavelength
E	Energy of the electron
T	temperature
h	Planck's constant
K	Boltzmann constant
QDs	Quantum dots
ν	Frequency
c	Speed of light
λ	Wavelength
AM	Air mass
I_D	Diode current

V	Voltage
I_0	Reverse saturation current
q	Elementary charge
I_{ph}	Photo-current
I	Cellcurrent
R_{sh}	Shunt resistance
R_s	Seriesresistance
J_{sc}	Short-circuit Current Density
G	Generation rate
L_n	Electron scatteringlength
L_p	Diffusion length of holes
V_{oc}	Open Circuit Voltage
ɳ	Electricalefficiency
FF	Form factor
p_m	Maximum power supplied by a cell
ϕ	illuminance received by the sample
p_i	Incident power
I_m	Maximum current
V_m	Maximum voltage
e	Electronicload
E_{ph}	The energy of the photon

Contents

List of Figures

Chapter 1

Chapter 2

Chapter 3

List of Tables

Chapter 2

Chapter 3

General Introduction

In the last few decades, semiconductor technology has attracted tremendous interest because of its exceptional properties. Since then,semiconductor materials are found virtually in most electronic and optoelectronic devices. They offer good light emission, detection and good doping conductivity control. It is also possible to change the electronic characteristics of a semiconductor by micro-and nano-fabrication processes. Particularly, the III-V semiconductors that are characterized by a direct gap and large electron mobility, such as GaNand InN, are very interesting in the field of optoelectronics. This discipline is based on the light-matter interaction, processes the conversion of electricity into light, or vice versa (light sources or detectors). The race for miniaturization and device integration led to the discovery of low-dimensional nanostructures such as quantum wells, quantum wires and quantum dots (QDs). The remarkable physical properties of QDs, which are derived from the zero-dimensional (0D) character of electronic states,have generated great interest both fundamentally and technologically. In these nanostructures, charge carriers occupy discrete energetic states: they are confined in the three directions of space. The formation principle of QDs consists of inserting small inclusions of a small gap material into a matrix of a larger gap material [1]. For there to be a quantification of the electronic states, the size of these nanostructures must be smaller than the de Broglie wavelength associated with the electron movement in the material,Imean a few tens of nanometers. These quantum dots are prime candidates for laser source and infrared detector applications [2,3]. For about fifteen years, the insertion of QDs into solar cell structures hasaroused great interest among the scientific community in the field of photovoltaic.

1.1 Introduction

The solar cell is a device for converting light into energy electric by a process called "photovoltaic effect" which is specific to some materials called "semiconductors". In this chapter that we will present the concepts necessary for understanding the solar cell.

First of all,wewilldiscuss about general information on semiconductors, next we will give notions on the production of photovoltaic electric energy, the basic components of a photovoltaic cell, the factors limiting the efficiency, and we will end with an equivalent electrical diagram of a cell photovoltaic.

1.2 General information on semiconductor

1.2.1 Definition of semi-conductor

Semiconductors are intermediate materials between metals and insulators. They are in principle insulators at temperature T=0K,because we can establish that the electrons of the valence layer completely occupy the allowed band highest energy (valence band).But the distance between this strip full of the first upper empty band in the energy diagram, that is, tell the width band gap E_g is weak while it is notable for insulators, and as soon as the temperature rises the semiconductors start to conduct electricity. Their resistivity varies between $10^{-3}\Omega.cm$and$10^{9}\ \Omega.cm$while that of metals is of the order of $10^{-6}\ \Omega cm$and that of the insulators can reach $10^{22}\Omega cm$ [4].

1.2.2 The electrical conductivity of a semiconductor

In a semiconductor, an atom makes covalent bonds with the neighboring atoms because of the electrons from the peripheral layer in order to ensure a cohesion of the crystal. These electrons are not free to participate in the creation of the electric power. But to produce electricity, just expose the semiconductor to an energy source (temperature or light) to break the covalent bonds and the electrons becoming mobile. Furthermore, and after the release electrons, the covalent bonds becoming pendant bonds called'' Holes'' or'' Gaps 'participate in the creation of electric current. These are

said to be holes are positive carriers and electrons are negative carriers. The increase of the temperature or the incident flux on the semiconductor induces the increase in carrier densities which explains the variation in its conductivity [5].

1.2.3 Type of semi-conductor

a- Intrinsicsemiconductor

An intrinsic semiconductor is an ideal material with no physical defect. Such a single crystal has a tetrahedral type structure. say that each atom is surrounded symmetrically by 4 other atoms.

At absolute zero temperature all the electrons are in the valence band and the width of the forbidden band is maximum. As the temperature increases, the width of the forbidden band decreases and certain electrons in the valence band increase their energies which allow them to immigrate to the conduction band. In the intrinsic semiconductor the energy level which is in the middle of the forbidden band is called the Fermi level [6]

b- Intrinsic concentration

At thermal equilibrium, the total densities of electrons and holes in the strip of conduction and the valence band respectively are given by the expressions following [7]

$$n = N_c \exp\left[\frac{E_f - E_c}{kT}\right] \quad 1.1$$

$$p = N_v \exp\left[\frac{E_v - E_f}{kT}\right] \quad 1.2$$

with

N_c : $Density\ of states\ of\ electrons\ in\ the\ conduction\ band.$

N_v: $Density\ of\ states\ of\ the\ holes\ in\ the\ valence\ band.$

E_c: $Energy\ of the\ conduction\ band.$

E_v: $Energy\ of\ the\ Valence\ band.$

E_f: $Fermi\ energy.$

An intrinsic semiconductor is a material that has no foreign atom (impurity) which causes a change in the densities of the carriers in both bands. The only change we can notice in this semiconductor ideal, is due to the transitions of electrons from the valence band to the band of conduction under thermal or light excitation.

In this type of electrically balanced semiconductor I mean that the holes and the electrons have the same density ($n = p = n_i$), and after excitation we find these carriers in the form of electron-hole pairs. We can get the concentration intrinsic and the Fermi level intrinsic by the following equations:

$$n_i = [N_c N_v]^{\frac{1}{2}} exp\left[-\frac{E_g}{2kT}\right] \quad 1.3$$

$$E_{fi} = \frac{1}{2}[E_v E_c] + \frac{3}{4} kTLog\frac{M_h}{M_e} \quad 1.4$$

with

M_e= Effective mass of electrons.

M_h=Effectivemass of the holes.

As a result, the intrinsic Fermi level is always very close to the center of the prohibited band. In the case of a non-degenerate semiconductor with thermal equilibrium:

$$p = p_0 , n = n_0 , p_0 . n_0 = n_i^2 \quad 1.5$$

$$n_0 = n_i \exp\ [-\frac{Ei-Ef}{kT}] \quad 1.6$$

$$p_0 = n_i \exp\ [-\frac{E_f-E_i}{kT}] \quad 1.7$$

1.2.4 Different types of doping

In the intrinsic semiconductor the creation of positive carriers and negative by a thermal increase or a light excitation to modify the conductivity cannotbevery useful, because the electron-hole pairs recombine with the decrease or absence of energy sources. So, adding atoms foreigners is necessary to facilitate the mobility of carriers in the crystal lattice. this procedure is called "Doping" and the semiconductor becomes extrinsic. there are two types of doping in semiconductors [7]

a- N dopedsemi-conductor

In an N doped semiconductor, the concentration of electrons is largely greater than the concentration of holes. We generally introduce phosphorus, Arsenic or Antimony to make the electron density important by compared to that of the holes. Take for example the case of Silicon in which introduces Arsenic (which has 5 electrons on the outer layer). In the band prohibited silicon Arsenic intervenes to create a very close donor impurity of the conduction band. For temperatures above $0\,°\,K$, atoms arsenicisionized which amounts to passing the electron from the donor level to the conduction band. The donor concentration will therefore be higher than that acceptors $\langle N_d - N_a > 0 \rangle$ which corresponds to the definition of a semiconductor doped N. At room temperature, almost all donors are ionized and if the concentration of donor atoms is,the density of the free carriers of the semiconductor will be:

$$n = n_0 + N_d \qquad 1.8$$

with

n_0: is the density of electrons generated by the bond breaking process covalent which generates electron-hole pairs.

b- dopedsemi-conductor

It is a semiconductor whose hole concentration is much higher than the electron concentration. We introduced generally Boron, Aluminum, Gallium or Indium, let's take the case of Silicon in which we introduce Boron. We associate with the Boron a level acceptor in the prohibited band very close to the valence band. Of the same as for the n doped semiconductor, the hole concentration of the semi driver will be:

$$p = p_0 + N_a \qquad 1.9$$

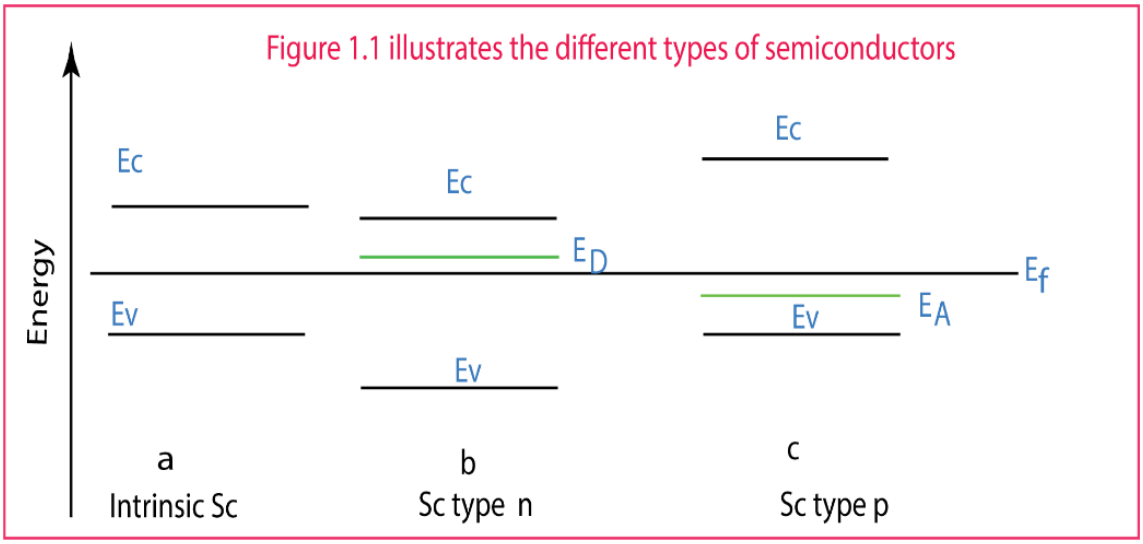

*Figure 1. 1*Shows the different types of semiconductors [53]

c- Charge density in a semiconductor

If we consider a Semiconductor with a density of atoms donors and a density of acceptor atoms, we can estimate that at the temperature ordinary all the impurities are ionized. This results in the following statement of charges:

$$n + N_a = p + N_d \qquad 1.10$$

In the case of n or p doped semiconductors the relation is simplifies when taking into account the orders of magnitude of the different concentrations.

- N doped Semi-conductor

$$N_a = 0 \; et \; N_d \gg p \longrightarrow n \approx N_d$$

The electrons are the majority carriers. The density N_d^+ of ionized donors is written:

$$N_d^+ = \frac{N_d}{1+2\mathrm{Exp}\left(\frac{E_f - E_d}{kT}\right)} \qquad 1.11$$

Ed: *being the donor energy level*

- P doped Semi-conductor

$N_d = 0\ et\ N_a \gg n \longrightarrow p \approx N_a$The holes are the majority carriers, the densityN_a^+ of ionized donors is written

$$N_a^- = \frac{N_a}{1+\frac{1}{4}\mathrm{Exp}\left(\frac{E_a - E_f}{\mathrm{kT}}\right)} \qquad 1.12$$

with

$E_a\ being\ the\ accpetor\ energy\ level$

Since the semiconductor material is generally neutral, the equation of electrical neutrality is written:

$$n + N_a^- = p + N_d^+ \qquad 1.13$$

d- Law of mass action

law of mass action links, at a temperature, the density of carriers (electrons and holes) at the intrinsic density of the semiconductor. It is expressed by:

$$n.p = n_i^2 \qquad 1.14$$

We deduce the concentration of the minority carriers of Semi n-doped and p-doped conductors:

- Holes in an n-doped semiconductor

$$p_n = \frac{n_i^2}{N_d} \qquad 1.15$$

- Electrons in a p-doped semiconductor:

$$n_p = \frac{n_i^2}{N_a} \qquad 1.16$$

1.2.5Current in the semiconductor

The currents in the semiconductor result from the displacement of the charge carriers, electrons and holes, under the action of different forces. The origin of these forces is an electric field (conduction current) or a gradient of concentration (diffusion current).The conduction current is the current that is encountered in the metals and which is proportional to the electric field:

$$\vec{J}_{cn} = q.n.\mu_n.\vec{E} \qquad 1.17$$

$$\vec{J}_{cp} = q.p.\mu_p.\vec{E} \qquad 1.18$$

with

μ_n : Mobility of electrons.

μ_p : Mobility of holes

The total current is then written:

$$\vec{J}_{tot} = q\left(n\mu_n + p\mu_p\right).\vec{E} = \sigma\,\vec{E} \qquad 1.19$$

with

$$\sigma(T) = q(n\mu_n(T) + p\mu_p(T)) \qquad 1.20$$

$$\sigma(T) = 1/(q(n\mu_n(T) + p\mu_p(T)) \qquad 1.21$$

Consider a doped semiconductor with varying hole concentration along an axis. The density of diffusion current at a point of abscissa is:

$$JD_p = -qD_p\frac{dp(x)}{dx} \qquad 1.22$$

Excess carriers tend to give themselves a uniform concentration. It is the same in the case of concentration electrons and we have:

$$JD_p = -qD_p \frac{dp(x)}{dx} \quad 1.23$$

with

D_n: Electron scattering constant.

D_p : Hole diffusion constant.

When the two phenomena exist simultaneously the total density of current for electrons and holes is given, explaining the relation of dependence on temperature, by:

$$J_n = q.n.\mu_n.E + q.D_n \frac{dn}{dx} \quad 1.24$$

$$J_p = q.n.\mu_p.E + q.D_p \frac{dp}{dx} \quad 1.25$$

These relations are valid for sufficiently weak electric fieldsso that the speed of the carriers remains proportional to the field. Total currentis then written:

$$J_{tot} = J_n + J_p \quad 1.26$$

The constants and are linked to mobility and by Einstein's relation:

$$\frac{D_p}{\mu_p} = \frac{D_n}{\mu_n} = \frac{kT}{q} = V_t \quad 1.27$$

1.3 Production of photovoltaic electrical energy

1.3.1 Solar radiation

The radiation emitted by the sun contains electromagnetic waves part of which, called solar radiation, keeps reaching the limit of the Earth's atmosphere. Because of the value taken by the temperature surface of the sun about 5800K, the energy of electromagnetic radiation transmitted to the earth mainly comes from the emission of light waves which located in the visible (between 0.4 and 0.7µm wavelength approximately) and the near infrared (between 0.7 and 4µm approximately).

This energy, averaged over a year and over the entire upper limit of the atmosphere, corresponds to an illumination of some 340 W/m². But on this amount of light that brings the sun in the earth-atmosphere system, about 100 W/m² are reflected towards space, the rest is absorbed one third by the atmosphere and two thirds by the surface terrestrial [10].

First, almost a quarter of this incident illumination is reflected in space through the atmosphere: such a reflection is essentially the result of clouds (around 65Wm^{-2}), the rest being due to other atmospheric constituents –gas and aerosols which reflect about 15 W/m². In addition, the atmosphere and its clouds absorb by absorption about 80W/ m2on the solar illumination: remain therefore approximately 180 W/m² which reach the Earth's surface at the end of a transmission of which about two thirds are done directly, the rest by diffusion down, it is thanks to this diffuse radiation that we can see continuously during the day, even when the clouds hide the sun. We are witnessing a fairly complex process of interaction between diffusion towards the low and reflection: the earth's surface, having a high medium albedo (the albedo is the fraction of incident radiation scattered or reflected by an obstacle), should return about 50 W/m² of the approximately 180 W/m² incidents to the atmosphere; but in fact most of the light it reflects comes back to it early or late by diffusion downwards from the atmospheric medium and is added partially to the 130 W/m² of solar radiation not reflected on contact. Although there are not in reality two separate instants for absorption by Earth's surface, but a continuous phenomenon of absorption of radiation we can summarize the previous process by saying that everything happens as if the 50 W/m² reflected by this surface were distributed between $20Wm^{-2}$ definitively returned to the interplanetary space after diffusion upwards to through the atmosphere and 30Wm-2 returning to the earth's surface after diffusion deferred down. These 30Wm-2 are added to the 130Wm-2 initially not thought to make up approximately 160 W/m² almost half solar radiation -absorbed by the earth's surface. By bringing all the layers of the atmosphere under normal conditions

(P = 1013 mbar and T= 25°C), we defined a standard atmosphere of vertical thickness average of 7.8 km taken for unit reference and formed of flat layers and laminates composed of various gases such as nitrogen (6,150 m layer), oxygen (1650 m), argon

(74 m), carbon dioxide (24 m) ... Water is represented by a layer of variable thickness of a few tens of meters for steam and a few centimeters for the liquid. From there we introduce the notion of mass air which allows to take into account the thickness of the atmosphere traversed by the sun's rays according to the inclination of the sun Figure 1. 2. It corresponds to the loss of solar energy by absorption atmospheric. The air mass is expressed as a multiple of the route crossed at a point at sea level, the sun being directly above the ground.

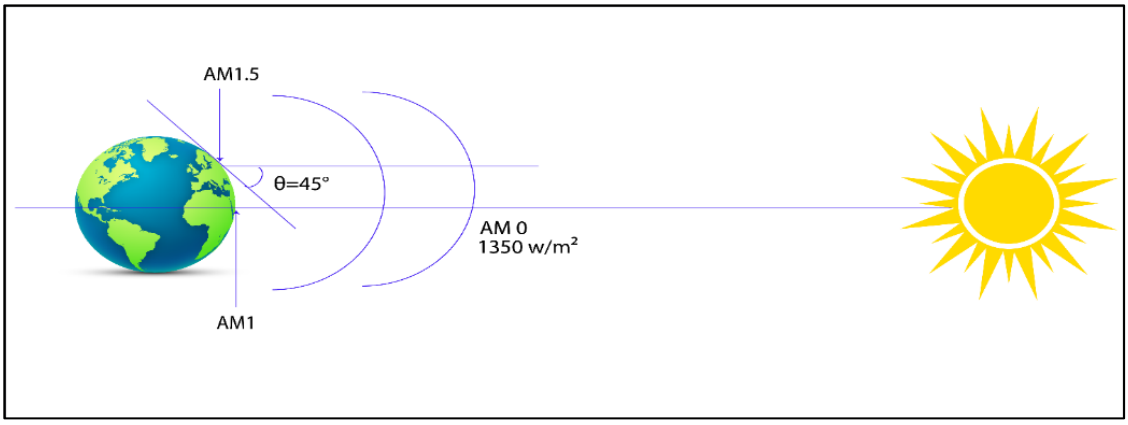

*Figure 1. 2*Standard for measuring the spectrum of light energy emitted by the sun concept of convention AM [53]

At each point, the value of the air mass is given by equation:

$$\mathrm{AM} \approx \frac{1}{Sin\theta} \qquad 1.28$$

Where the angle θ is the solar elevation I mean the angle in radians between the solar radiation and the horizontal plane. The solar spectrum AM 0, corresponds to a zero-air mass for solar irradiation beyond the incident atmosphere normal. For a clear sky with the sun above, we have the radiation of the mass of air "1" (or AM_1),AM_2 when there is an inclination of 30 °, the solar illumination arriving on earth with an angle of 48 ° is $1000W/m2$ (i.e. 100mW/cm2) with an air mass $AM_{1.5}$ [10]. The solar spectrum AM1.5 is composed of 3 ~ 4% of ultraviolet light (<390 nm), 45% visible light (390-750 nm) and 52% infrared light [Close IR (750-1400) = 38% and Far IR (> 1400) = 14%]. Figure (1.4) shows that the illumination is maximum between 450 and 700nm. Among the major

factors which are involved in an efficient photovoltaic conversion, there is the absorption of white light received on earth. It is important to understand the two aspects covered by the concept of number of air mass. On the one hand, it characterizes the power carried by the solar radiation (1353Wm-2 for AM 0 ,833Wm-2 for AM1.5 and other part, it is used to define a reference spectrum to calibrate the standard cells intended to qualify the performance of photovoltaic devices. So, the conditions cell qualification standards are AM 1.5 spectrum, incident power 1000W$m^{-2}$and a temperature of 25 ° C. Unless otherwise stated, it is for such conditions that performance and specifications must be provided of a given photovoltaic device.

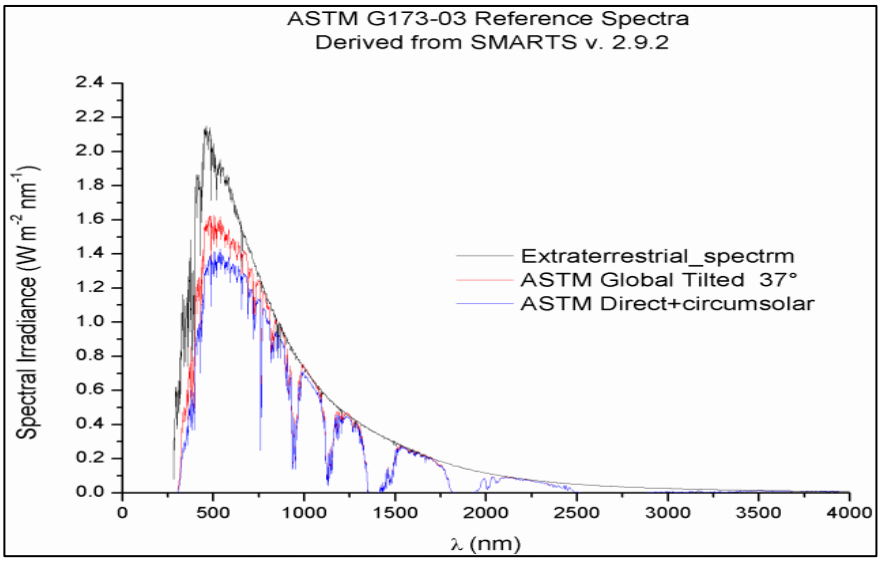

*Figure 1. 3*Representation of the solar spectrum, outside the atmosphere AM0, at the level of sea with sun at zenith AM1, with sun at 48 ° to the equatorAM1.5 [53]

1.3.2 Light absorption and reflection

The absorption of sunlight by the material being probably the main mechanism of the generation phenomenon. The majority of semi- Basic conductors of solar cells adequately absorb the visible spectrum. In fact, we always use semiconductors with a

coefficient high absorption. The absorption rate of photons by a semi-material conductor is directly linked to the energies of the incident photons.

Absorption only takes place if the energy of these photons is equal to or greater to the energy of the semiconductor bandgap E_g. The photons that don't do not meet this condition (E_{ph}<E_g)will not be absorbed and will not contribute not to photovoltaic conversion. If there is an energy greater than E_g. Photon2 from the diagram in figure (1.4) generates an electron-hole pair at higher level, but the excess energy is lost by a spontaneous de-excitation process which produces heat and brings its energy back to the lower band levels and knowing that each absorbed photon creates only one electron-hole pair [11].

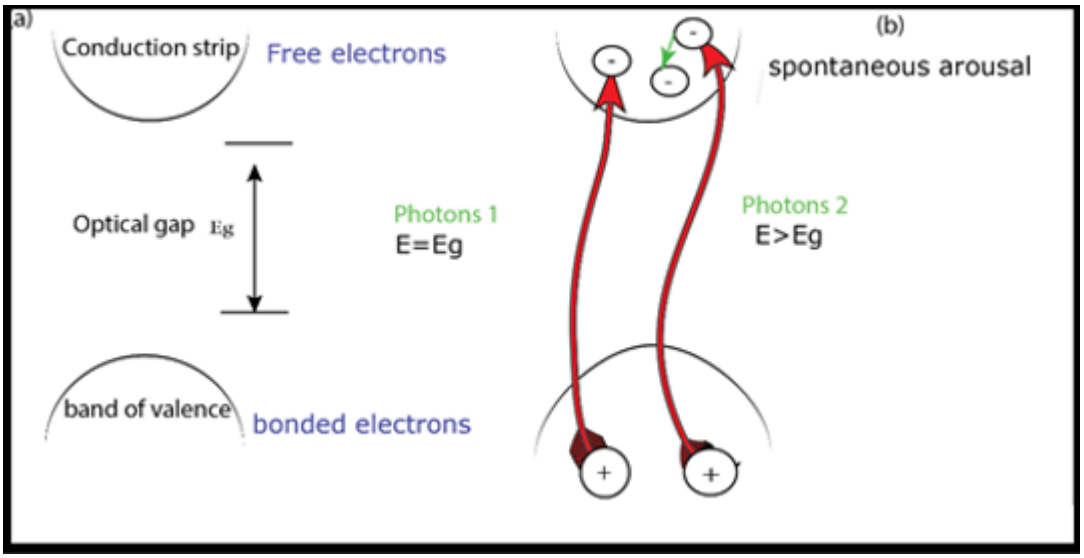

*Figure 1. 4*Energy diagram of semi-conductor a) in the dark. B) under illumination [53]

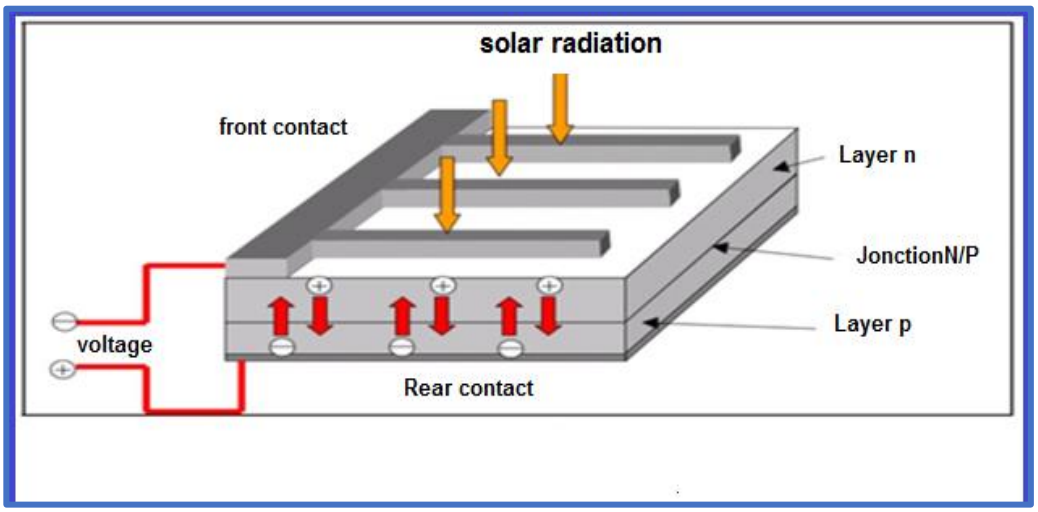

Figure 1. 5 : Cross section of typical photovoltaic cell [53]

1.3.3 The photovoltaic effect

a- Photovoltaicenergy

Photovoltaic energy (PV) is the direct transformation of light into electricity. It is not a form of thermal energy. It uses a solar cell to directly transform solar energy into direct current. The photovoltaic effect was discovered by E. Becquerel in 1839: he discovered that certain materials delivered a small amount of electricity when they were exposed to light. Albert Einstein explained the photoelectric phenomenon in 1912, but it was not until the early 1950s that scientists deepen and exploit this physical phenomenon [12]. The use of solar cells began in the forties in the space domain. Post-war research has improved their performances and their sizes, but it will be necessary to await the energy crisis of 1970s for governments and industrialists to invest in photovoltaic technology and its terrestrial applications.

b- The photovoltaiccell

To obtain a photovoltaic cell it is necessary to make a diode structure, that is to say make a junction of the p-n type. The electric field that reigns at the junction of these two differently doped zones separates the electric charges photo-generated by sunlight (pairs of electron-holes) and ensures their evacuation of the crystal the electrons through the cathode and the holes through the anode [13].

c- Photovoltaicprinciples

The transformation of solar energy into electrical energy is based on the three

following mechanisms [14]:

- absorption of photons (whose energy is greater than the Gap) by the materialconstituting the device;
- converting photon energy into electrical energy, which corresponds to thecreation of electron / hole pairs in the semiconductor material;
- collecting particles generated in the device.

The material constituting the photovoltaic cell must therefore have twoenergy levels and be conductive enough to allow the flow of currenthence the interest of semiconductors for the photovoltaic industry. In order to collect the generated particles, an electric field allowingdissociate the electron / hole pairs created is necessary. For this we use the mostoften a p-n junction. Other structures, such as heterojunctions andSchottky diodes can also be used.The operation of the photovoltaic cells is illustrated in the figure (1.6) and Figure (1.7).

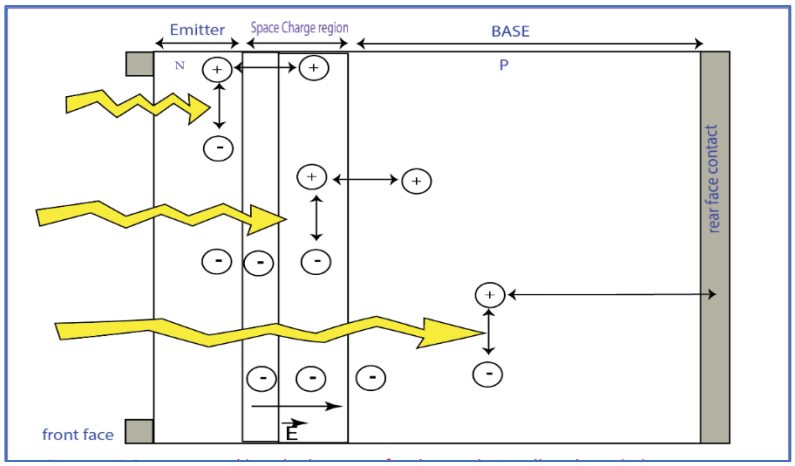

Figure 1. 6 : Structure and band diagram of photovoltaic cell under enlightenment [53]

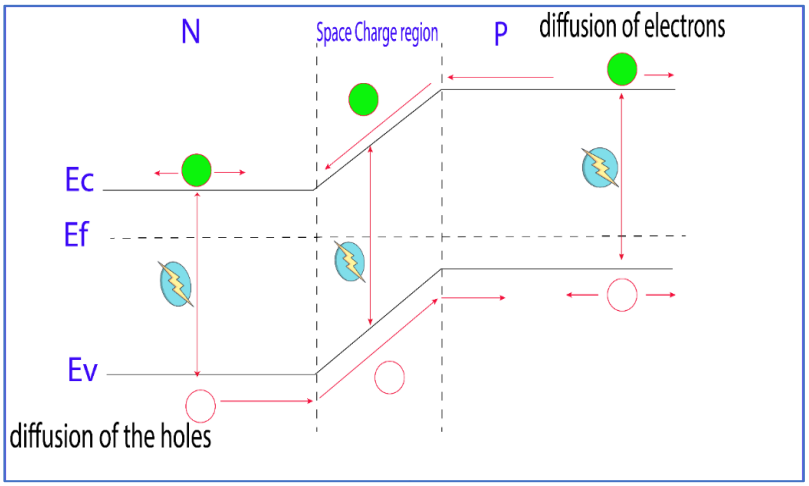

Figure 1. 7 :Structure and band diagram of photovoltaic cell under enlightenment [53]

Incident photons create carriers in the n and p zones and in the zone space charge. Photocarriers will behave differently depending on the region [11]

- in zone n or p, minority carriers who reach the load zone of space are "sent" by the electric field in zone p (for holes) or in zone n (for electrons) where they will be the majority. We'll have a scattering photocurrent.
- in the space charge area, the electron / hole pairs created by the incident photons are dissociated by the electric champ: the electrons go to region n, the holes to region p. We will have a photocurrent of generation.

These two contributions are added to give a resulting photocurrent Iph. It is a current of minority carriers. It is proportional to the light intensity.

1.3.4 The basic components of a photovoltaic cell

Although different structures are possible for the development of cells photovoltaic, similar parts are present in each component.

a- Passivation of the front and rear faces

The surface of the semiconductors contains a high density of defects (pending connections, impurities, etc). resulting in significant losses related to the surface recombination. Passivation involves improving the qualities material surface and volume by neutralizing the effects of its electrically active faults. Various passivation layers are used in photovoltaic but the main ones are thermal silicon oxide (SiO2), nitride hydrogenated silicon (SiNx: H) and tin dioxide (SnO2) [15].

b- Anti-reflectivelayer

To minimize the reflection of light, an anti-reflective layer (CAR) is used. The principle of action of anti-reflective layers is based on the interference of light beams in thin dielectric layers. Ifthe thickness of the dielectric layer is equal to:

$$dVar = \frac{(2.N+1)\lambda}{4*\eta_{CAR}}\text{, N=0,1,2,3}$$

We will get the cancellation of the reflected beams at the air / CAR interface and CAR / semiconductor. For high efficiency photovoltaic cells,a double anti-reflective layer is used (with two different dielectrics). Different CARs are used in photovoltaics: TiO2, SiO2, ZnS, MgF2, SiNx, [15] .

c- Surface texturing

Texturing is used to decrease the reflectivity of the surface of the cell. This operation aims to develop micrometric relief on the surface, generally pyramidal in shape. The wavelength of the incident light being smaller than the dimensions of the structures thus produced, the incident rays follow the laws of geometric optics. The insertion presents the principle of multiple reflections specific to texturing. The relief of the surface causes a drop reflection on the front: a ray arriving at normal incidence relative to the plan of the cell on a pyramid will be reflected on the face of an adjacent pyramid, this double reflection on the pyramids decreases the coefficient of total reflection, which no longer worth R but R^2 [15].

On the other hand, a normal radius of incidence will be transmitted in the cell with a refraction angle θ different from 0 °. The path of this radius within the material will be so increased by a factor 1 / sin θ compared to the case of a flat surface and perpendicular to the illumination, which will increase the share of photons absorbed by the material. Finally, the texturing of the surface leads to trapping most important of the light entering the cell. On the back of the cell, there is a critical angle of incidence θ_c from which the ray is fully reflected and extends its path within the semiconductor, again increasing the absorption photons.

This phenomenon is particularly important in the case of cells of low thickness, and can be reinforced by a texturing of the rear face and / or an anti-reflective layer on this same face. Different processes are used to texture the surface of semiconductors: chemical attacks on the surface (KOH, NaOH, acids), mechanical texturing (cold rolling under a serrated comb), texturing laser [12].

d- Contacts front and rear

The metal contacts on the substrate are used to collect the current of carriers photo generated. The contacts must be ohmic, i.e. the characteristic I = f (V) of the contact must be linear. Contact resistance is a very important parameter important. The high resistance of the contacts increases the series resistance of the cell and lower form factor and yield. Different methods are used to make the contacts. As part of industrial photovoltaic cells in Multicrystalline silicon, the contacts are generally made by screen printing. For the high efficiency photovoltaic cells, sputtering or vacuum evaporation is used [15].

e- The rearelectricfield

The Back Electric Field (BSF) consists of creating a potential barrier (for example, junction (P+ , P-) on the rear face of the cell.

to ensure passivation. The potential barrier induced by the difference in doping level between base and BSF tends to confine minority carriers in the base.Theseare therefore kept away from the face which is characterized by a very high recombination speed. The BSF does still the subject of much research because the thickness of the plates is constantly reduced in order to save raw material.

1.3.5 Electrical characteristic of a photovoltaic cell

In the photovoltaic cell, two currents oppose each other, the current of illumination (photocurrentI_{ph}) and a current of the diode called current of darkness (I_{dark}), which results from the polarization of the component. The resulting current

I(V) is[13]:

$$I(V) = I_{dark}(V) - I_{ph} \quad 1.29$$

with:

$$I_{dark}(V) = I_s(e^{\left(\frac{qV}{nkT}\right)} - 1) \quad 1.30$$

$$I_{ph} = Aq.\phi.\left[1 - \left(\frac{e^{-aw}}{1+aw}\right)\right] \quad 1.31$$

with:

q: Elementary charge: $q = 1.6.10^{-19}C$

V: Voltage across the junction.

k: Boltzmann constant:$K = 1.38\,.10^{-23}j.K^{-1}$

Φ: Incident flow.

T: Temperature in (K).

A: Surface the PV cell.

(I_s) the saturation current of the diode. n is the ideality factor for the diode, function of the quality of the junction (equal to 1 if the diode is ideal and equal to 2 if the diode is real).

The characteristic of a cell in the dark is identical to that of a diode. Under illumination, the current-voltage characteristic has the appearance presented in the Figure (1.8).

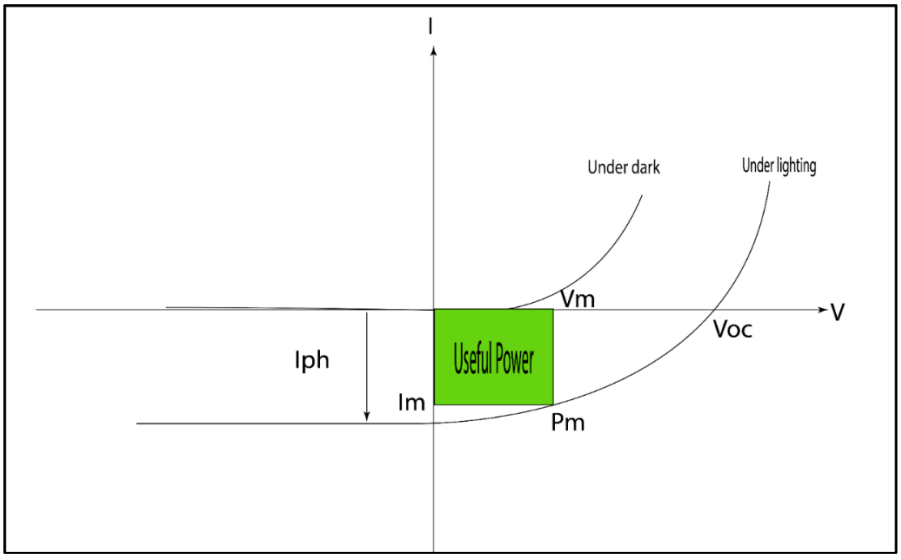

Figure 1. 8 : Current and Voltage characteristic in darkness and under illumination for a photovoltaic cell [53]

with

I_{sc}: Short-circuit current (obtained for V = 0).

V_{oc}: Open circuit voltage (obtained for I = 0).

I_m: Current at the maximum operating power of the PV cell.

V_m: Voltage at the maximum operating power of the PV cell.

η : Conversion efficiency.

FF: Fill factor.

$$\eta = \frac{maximum\ electrical\ power\ supplied}{incident\ solar\ power} \tag{1.32}$$

$$\eta = \frac{V_m I_m}{P_i . \mathrm{A}} = \frac{\mathrm{FF}. V_{oc} . I_{sc}}{P_i . \mathrm{A}}$$

P_i: Illumination power received per unit area.

$$FF = \frac{V_m . I_m}{V_{oc} . I_{sc}} \tag{1.33}$$

1.4 Factors limiting the efficiency

In practice, the conversion of light energy into electrical energy is not total. Different losses influence the performance of a cell. They are in most cases due to the nature of the material and the technology used. These losses are discussed below:

1.4.1Physical losses

All photons with a wavelength greater than that associated at the Gap of the semiconductor ($\lambda_{ph} > \lambda_g$), cannot generate an electron-hole pair, and are therefore lost. A more detailed model of the phenomenon, however, allows consider the absorption mechanisms.

Photons of energy greater than Gap can only generate one electron hole pair. Excess energy is lost in the form of heat.

The voltage factor $\left(\frac{qV_{oc}}{E_g}\right)$, is the ratio of maximum energydeveloped by the Gap energy cell. The voltage across the cell is not that a fraction of the energy of the Gap mainly

because of the fall in potential at the contacts and the junction; the best values obtained from Vco areof the order of 700mV [17].

The form factor cannot exceed 0.86 [18], because the current-voltage are generated by Boltzmann equations in exponential form($exp^{(qv/kT)}$), so there are no rectangular curves I(V), even in the case of an ideal cell .This setting also depends the design of the cell, the quality of the junction of the materials used, theresistivity of metal contacts, etc. These physical factors being considered as limiting for a structure given photovoltaic cells, technological factors are the only one factors who can improve the cell's performance.

1.4.2Technological losses

The efficiency of the photovoltaic cell depends basically on the number of incident photons. This amount of energy is limited by the reflection coefficient of the surface of cell R, which weights all the photocurrent equations of generation by a factor (1-R), the reflection coefficient can be optimized by the implementation of appropriate surface treatments and anti-reflective coating. The metal contacts present on the front face of the cell in order to collect the carriers, cause power losses because they cover parts of the cell receiving surface (shadow effect). The width of metal creates a compromise between losses due to partial coverage of the issuer and losses. Form factor FF caused by series resistance related to the width of the metallization. There are photons, having the energy to create an electron-hole, but which pass through the thickness of the cell without being absorbed. This number of photons become important especially in thin thick cells (<100 µm). this phenomenon reduces the absorption efficiency, and can be reduced by using areflectivelayer on the rear face of the cell (called rear reflector or"BSR" rear mirror) [19].The collection yield, is the ratio between the number of charge carriers actually collected, and the number of photogenerated carriers. Indeed, some carriers recombine on the surface or in the volume of the photovoltaic cell. This phenomenon is directly linked to the lifespan of minority holders (the average time between generation and recombination of a minority carrier). Also;

it is possible to improve the collection by the use (dissemination) of aback field in the case of the NP structure (BSF) [20].

These phenomena can be optimized using the technologies of manufacturing of photovoltaic cells.

1.5Equivalent electrical diagram of a photovoltaic cell

Figure (1.9) presents a model of the photovoltaic cell, taking into account factors limiting the efficiency, we find the current generator (Iph), which translates the photogenerated current as well as the additional resistances Rs and Rp, and two diodes and D1 and D2 and R_L. is the load resistance [21].

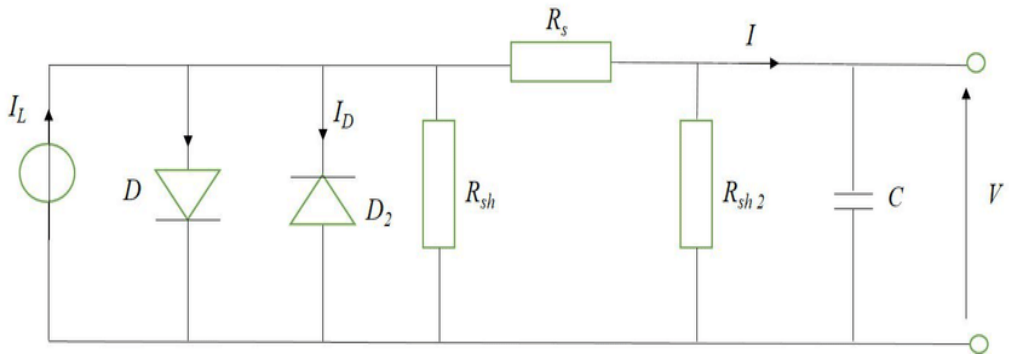

*Figure 1. 9*Equivalent diagrams of photovoltaic cell [53]

$$I = I_1 + I_2 + I_P - I_{ph} \qquad 1.34$$

$$I = I_{s1}\left(e^{\frac{q(V-I\mathrm{R_S})}{\mathrm{n_1}kt}} - 1\right) + I_{s2}\left(e^{\frac{q(V-I\mathrm{R_S})}{\mathrm{n_2}kt}} - 1\right) + \frac{V-I\mathrm{R_S}}{\mathrm{R_p}} - I_{ph} \qquad 1.35$$

with :

$$R_{p=}\frac{(R_{sh}R_{sh2})}{R_{sh}+R_{sh2}}$$

Rs the series resistance models the resistance of the different layers of the cubicle (transmitter, base and metal contacts). To limit the impact of this resistance on the cell current, its value must be as low as possible. This can be achieved by optimizing the metal / semiconductor contact surface and by reducing the resistivity of the material used. However, too high doping leads to an increase in the recombination of carriers.R_p parallel resistance (short-circuit) meanwhile, the presence current through the transmitter caused by a fault. This is the case when the diffusion of metallic contacts at high temperature punctures the transmitter. She can be due to a short circuit around the edges of the cell. This value should be the highest possible. The first diode which has an ideality factor n_1≈1 corresponds to the current ofbroadcast in the base and the cell transmitter I_1. This is the saturation current of this phenomenon. I_p is the generation-recombination or tunneling current in the area of space charge, with I_2 the saturation current of this phenomenon and n_2≈2 the ideality factor for the second diode.

1.6Conclusion

In this chapter, we have recalled some notions about semi- conductors, solar radiation and the mechanisms induced during its interaction with semiconductor materials. We have next explained the operation of photovoltaic cells and their characteristics main parameters as well as the parameters limiting their conversion efficiency with a modeling of the PV cell by an electrical circuit.

Chapter 2 Study of the Structure InGaN/GaN and quantum dots

2.1 Introduction

This chapter presents the material of gallium-indium nitride (InGaN) which is at the center of this work. This material is a semiconductor belonging to the category of nitrides-III, that is, composed of nitrogen and elements from column III of Mendeleev's table, at know the bore, aluminum, gallium, indium and thallium, Nitride gallium-indium is an alloy between gallium nitride (GaN) and indium nitride (InN).

InGaN is currently emerging as the most promising material for applications photovoltaic. It is actively studied because it represents a new category of materials with unique properties: A large direct prohibited bandgap energy, allowing it a broad spectral coverage, strong interatomic bonds or even a high thermal conductivity. Its gap is modular with the substitution rate of Indium in the alloy.

2.2 Description of Gallium-Indium Nitride

Nitride gallium-indium composed from the combination of two elements situated in column 3 of Mendeleyev table with the third element of the column 5, it means (Ga) , Indium(In) and the Nitride (N) We can find also other alloys like (AlGaN) or (BN)…These Materials are divided to two categories the first called Zinc Blende and other Called Wurtzite refers to their Structures crystallography[22].

2.3 Structural features

2.3.1 Crystal structure:

GaN and InN nitrides are essentially present in two crystalline forms: Hexagonal structure "wurtzite" and cubic structure "zinc -blende". Under ambient conditions, the structure of III-nitrides is wurtzite, a structure Hexagonal, this structure is defined by three parameters, the width of a hexagonal side (at). The height of the elementary lattice c, and the internal parameter u describing the separation of Subnetworks of

anions (N-3) and cations (Ga^{+3}) along the c axis [23]. The latter is defined as the length of the cation-anion bond divided by c. It is equal to 0.375 for an ideal wurtzite crystal.

The second zinc-blende structure consists of two cubic sub-networks with faces centered, one consists of an element III and the other of an element V, the two sub-networks being shifted by a quarter of the main diagonal, i.e., "a" being the length of the cube, Le Table 2.1 presents the lattice parameters of GaN and InN nitrides for both structures. This structure, for its part, can only be obtained under conditions of good growth. particular, it is thermodynamically unstable. In nitrides the bonds are covalent type exhibiting partially ionic properties, such as one of the four bonds receives two electrons from the element V.

Materials	a(Å)	C (Å)	U(Å)
GaN	3.189	5.185	0.376
InN	3.54	5.707	0.377

Table 2. 1GaN and InN settings

This structure is shown in Figure 2.1 Where Gallium is represented by the large spheres and nitrogen by small. However

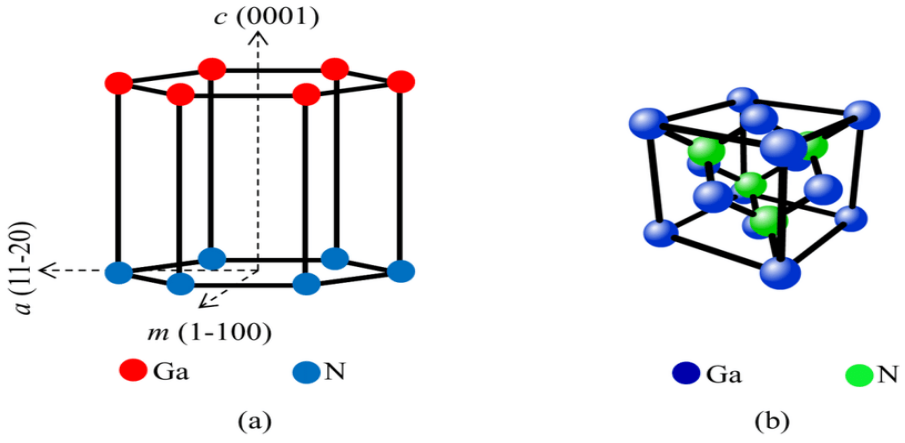

*Figure 2. 1*Wurtzite Structure for GaN according to (a) 0001 A (b) 1120 (c) 1010 [62]

However, even if the wurtzite structure is the most used, it turns out that the zinc-shielded presents more interesting electrical and optical properties such as a higher

mobility or better optical gain, but very complex production of this structure significantly reduced the use of the latter [24].

2.3.2 Electrical properties:

The electrical properties of a material come from its bandgap energyEg, and of its carrier density. Before detailing these values for InGaN, we will recall quickly some essential notions of physics. The bandgap energy is defined as the energy difference between the top of the valence band and the bottom of the band conduction.

2.3.3 Electronic properties

a- Contaminent of carriers

The De Broglie wavelength λ_β associated with the conduction electron, of effective mass

M $*$ and thermal energy kT is written:

$$\lambda_\beta = \frac{2\pi h}{(2m_e)K_\beta T} \qquad 1.36$$

Where is the quantized energy associated with the system? The second term is kinetic energy

due to the free movement of the electron in directions without confinement et k the wave vector associate $\hbar$ = h⁄2π.

If a semiconductor material having an optical gap E_{g1} called an active layer is surroundedby a larger Eg2 gap material, called a barrier, this creates areas in which thecarriers (electrons and holes) are confined with quantified energies. This quantification ofthe energy, differentdepending on the confinement, offers the possibility of creating objectsvery different characteristics. So,we are talking about 2D confinement in a well structurequantum. Theenergy of the electrons in these structures is then of the type:

$$E_{(K_{II})} = \frac{h^2 k_{II}}{2m^*} = \frac{h^2}{2m^*}\left[K_x^2 + K_y^2 + \left(\frac{n_z}{l_z}\right)^2\right] \qquad 1.37$$

n_z: quantum number.

Where $(\overrightarrow{k_{II}})$ the wave vector in the plane. The density of state, in a 2D system, is a function

staircase whose expression

is as follows:

$$D(E) = \Sigma_n D_n(E) \qquad 1.38$$

To increase the confinement of carriers of quantum wire-type structures, two of which dimensions correspond to the DE Broglie wavelength allow confinement of carriers in two directions of space (y and z for example). The density of state is proportional to$\frac{1}{\sqrt{E-E_n}}$as indicated in figure 2.2

$$D(E) = \Sigma_n D_n(E) = \Sigma_n \frac{1}{\sqrt{E-E_{n_z}-E_{n_y}}} \qquad 1.39$$

Pour E –E_{nz}- E_{ny}> 0

The energy of the carriers in these structures is of the form:

$$E_{(K)} = \frac{h^2 K_x^2}{2m_e^*} = \frac{h^2}{2m_e^*}\left[K_x^2 + \left(\frac{n_y}{l_y}\right)^2 + \left(\frac{n_z}{l_z}\right)^2\right] \qquad 1.40$$

where k_x is the wave vector associated with one-dimensional free motion 1D.

n_y, n_z: quantum numbers

Finally, 0D confinement in a structure of quantum dots allows them to confine carriers in all three directions of space; the spectrum of the density of state is entirely discretized in first approximation.

The density of states of quantum dots is written in the following form:

$$D(E) = \Sigma_n D_n(E) = \Sigma_n \delta \qquad 1.41$$

E_n: is theconfinement energy.

δ: is the Dirac function.

The energy of the carriers in these structures is:

$$E_n(k) = \frac{h^2}{2m^*}\left(k_x^2 + k_y^2 + k_z^2\right) = \frac{h^2}{2m^*}\left[\left(\frac{n_x}{l_x}\right)^2 + \left(\frac{n_y}{l_y}\right)^2 + \left(\frac{n_z}{l_z}\right)^2\right] \quad 1.42$$

n_x, n_y, n_z: quantum numbers

Electronic confinement in quantum dots brings about radical change the density of electronic states in relation to massive materials, quantum wells or even quantum wires. Indeed, the density of electronic states presents a discrete spectrum under the action of this confinement resulting from the discretization of the energy levels, as presented in Figure 2.2.

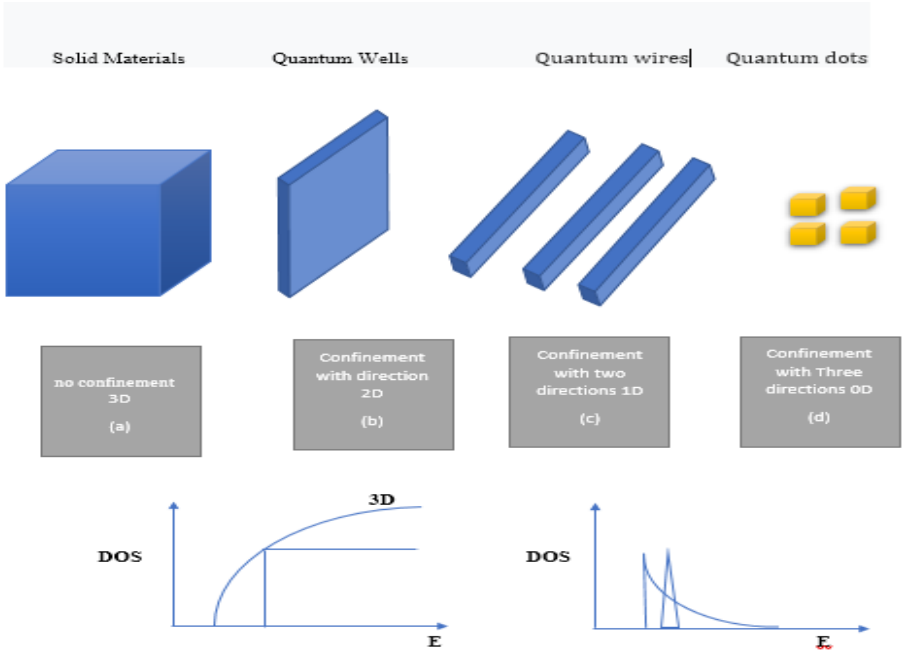

Figure 2. 2 : *Evolution of the density of states with the level of quantum confinement. (to anyone confinement, (b) confinement along one direction (2D system), (c) confinement along two directions (1D system) and (d) containment in three directions (0D system) [27,28].*

2.4 The Quantum Dots

2.4.1General concepts on quantum dots

A quantum dot, also called quantum point or by its English name (quantum dot), is a nano-crystal of semiconductor material whose dimensions are less than 10 nm.

Due to its size, it behaves like a potential well which confines the electrons and holes in the three dimensions of space [26], in a region of the order of wavelength of electrons according to DE Broglie, We mean a few tens of nanometers in a semiconductor.

This confinement gives quantum dots properties close to those of an atom, reason why quantum dots are also called "artificial atoms" [29].

The first 0D systems produced are spherical nano crystals of IIVI semiconductor in 1936 [31]. The first observations of the obtaining of quantum dots of III-V semiconductors (InGaN/GaN) date back to the 1980s [32]. This considerable attraction for quantum dot-type structures [33] are scientific and technological in nature. The interest science lies in the desire to understand the physics of nanostructures. Indeed, quantum dots lie at the intersection of the domain of condensed matter and quantum physics.

The technological interest comes from the potential applications of these nanostructures in high performance devices such as LEDs, lasers, optical memories [32, 34, 35] or still in quantum information [36] (because it is possible to generate quantum states usable in the transmission of information). In 2010, quantum dots are at the forefront of research in the field of semiconductors, in particular concerning transistors, LEDs, high-voltage photovoltaic cells.Efficiency [37, 38] and laser diodes [39]. A quantum dot can be imagined as a giant artificial atom [40] made up of thousands of real atoms. We will, through this part, describe some interesting properties that could result from the use of QDs as active area of a component

2.4.2Growth of quantum dots

A sample on which quantum dots have been grown has three elements: thesolid three-dimensional material, the buffering layer and the boxes themselves which confine the carriers in all three directions of real space.

There are several ways to achieve quantum dots, although each time they are to "reshape" pre-existing 2D layers. Among these techniques, we can cite the so-called of Stranski-Krastanov, which is the one we are going to use it for growing the boxes quantum. For the last few years, there are several methods for making box structures quantum.

a- The lithographymethod

The fabrication of quantum dots by lithography was the first method studied by Petroff et al for the production of III-V semiconductor nanostructures. This method is intensively studied because it is difficult to make small boxes and their surface had many flaws. The main drawback is the degradation of the properties optics of the structures to be developed and does not make it possible to obtain a high density of nanostructures. This technique requires very complex and expensive equipment [41].

b- The epitaxialgrowthmethod

The numerous studies in the growth of thin films have made it possible to distinguish three

epitaxial growth modes:

- The Volmer-Weber mode of growth is growth that is immediately

three-dimensional (3D), it takes a place when the adsorbed atoms will enucleate to form

aggregates [42].

- Frank-van der Merwe growth mode, in this mode is growth is two-dimensional (2D) or layer by layer due to the favorable interaction between the deposit and the substrate. Thus, the growth of the second layer will not begin until the end of the growth of the first [43].

Finally, we have the Stranski-Krastanov (SK) growth mode. This mode is particularly interesting for the formation of small islands where the growth is a combination of two previous modes: after a start of 2D growth, we observe a transition to a 3D growth with the appearance of 3D islands. It is based on the growth of one material over another

very different lattice parameters, particularly by molecular beam epitaxy (MJE).

c- Growth techniques

The main techniques currently used for the fabrication of quantum dots are vapor phase epitaxy which uses halides (Hybrid Vapor Phase Epitaxy:"EPVH"), vapor phase epitaxy by pyrolysis of organometallics (MetallorganicVaporEpitaxy phase "PVOME") and molecular beam epitaxy (MJE) (Molecular BeamEpitaxy MBE). The development of modern techniques for crystal growth and purification of semiconductors, has enabled the production of several binary and ternary alloys and quaternaries.

These alloys are characterized by the presence of stoichiometric coefficients. The extension will allow semiconductors to be considered whose bandgap will extend to values of 0.18at 2.42 eV. The results were long limited to the determinations of band structures and network settings depending on the composition. The quality of the materials was sufficient,

Gallium arsenide (GaAs) was in development in the early 1970s.

2.4.3 The strain

The most studied system is obtained by growth of InN: (with lattice parameter 6.058A) on GaN: (with lattice parameter of 5.653A). The lattice of the epitaxial material deforms elastically in the two directions parallel and perpendicular. In the case where the epitaxial layers are thin enough, the lattice of the epitaxial material deforms elastically so that the lattice parameter matches the parameter of the substrate in the direction parallel tothe interface. In the direction perpendicular to the growth interface the lattice deforms, stretching or compressing depending on whether the lattice parameter of the layer is smaller or larger than that of the substrate.

2.4.4 Bandgap energyin nitrides:

The Bandgap energy is 3.39 eV (366 nm) for GaN and 0.7 eV (1771 nm) for InN at room temperature (300 K) [46]. The main characteristic for which nitrides are so studied is their direct bandgap energy, including through their alloys. This allows for better conversion or issuance Efficiency of light, for photovoltaics or for LEDs, for example. In addition, their alloys cover almost the entire solar spectrum, from infrared (IR) to ultraviolet (UV).

These parameters for GaN and InN are collated in Table 2.2

	E_g(0K)	$\propto (\frac{meV}{K})$	$\beta(K)$	Eg(eV) at T=300K
GaN	3,507	0 ,909	830	3,44
InN	0 ,69	0 ,41	454	0 ,64

*Table 2. 2*Varshini parameter and bandgap energy at 0 and 300 K of the GAN and of the InN

Where the densities of states of GaN and InN are represented by the straight parts and the bands energies prohibited by the gray parties. The numbers represent the high points symmetry using the Rashba notation with the maximum of the valence bands taken as the benchmark of energies.

2.4.5 Interpolation

It is necessary to estimate the physical quantities of the alloy from the correspondent values to the basic binary materials that make it up. Using Vegard's interpolation line law, the physical parameters of ternary alloys can be extracted from those of the binary ones. In the case of a layer of pseudo morphic InGaN on GaN, the InGaNis tensile strain.

2.4.6 Lattice parameter

The respective lattice parameters of the InN and GaN are a_{InN}=6.058Å, a_{GaN}=5.653Å. The lattice parameter of In1-xGaxAs alloy is determined by the linear law of Vegard based on the proportion of Indium and the lattice parameters of the non-forced binary compounds InAs and GaAs [49]:

$$a.InGaN(x) = (1 - x).a.GaN + a.InN\,x \qquad 1.43$$

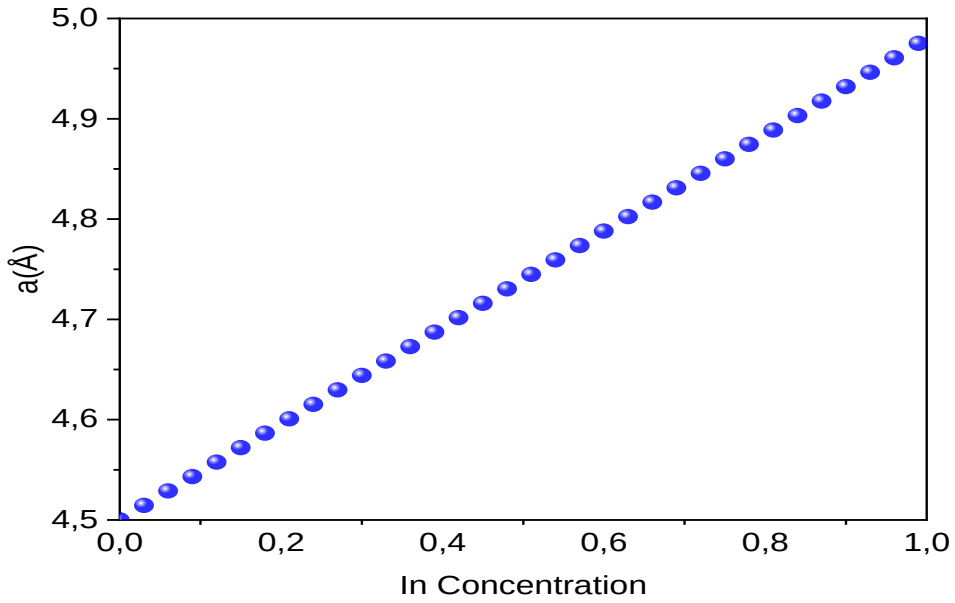

*Figure 2. 3*Variation of Lattice parameter according of In(x)Ga(1-x) N to Indium concentration

We have plotted the lattice parameter of InGaN as a function of the indium concentration in figure2. 3,we can see that indium has the effect of increasing the lattice parameter.

2.4.7 Parametric strain and the evolution of bandgap energy

For x values (indium concentration) during the epitaxy of in1-xGaxNon theGaN substrate, the connection of the lattice to the interface results in the existence of a transformation of the crystalline lattice. Fig 2. 4 Shows the variation of band gap energy and the variation of the strain according to the Indium concentration in InGaN alloy. This figure shows that a decrease in InGaN bandgap energy is accompanied by an increase in InGaN strain.

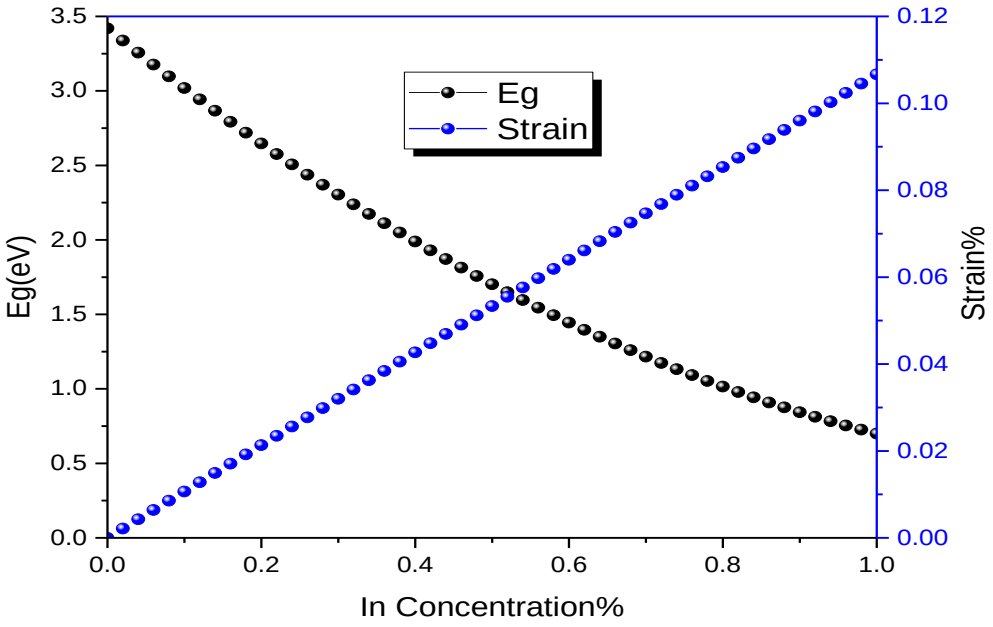

*Figure 2. 4*Variation of band gap and the variation of strain according to the Indium concentration

2.4.8 Evolution of the materials Gap ($In_xGa_{1-x}N$):

From the forbidden energy gaps of GaN and InN binary compounds, it is possible to determine the energy gap of InGaN using Vegard's law with a parameter of curvature. Vegard's law is an empirical law indicating that the values of the properties of an alloy (bandgap energy, lattice parameter, elastic constants, etc. [47,48]. We must then introduce a curvature parameter in the expression in order to follow the experimental data. Vegard's law with curvature parameter is defined by:

$$\mathrm{E_g}^{(InGaN)} = (1-x)\mathrm{E_g}^{(GaN)} + x\,\mathrm{E_g}^{(InN)} - b.x(1-x) \qquad 1.44$$

with:

x: the concentration of gallium in the $In_{1-x}Ga_xN$

$\mathrm{E_g}^{InGaN} =$ (: the bandgap energy of the InGaN [eV]. E

$\mathrm{E_g}^{GaN}$: the GaAs [eV] bandgap energy.

$\mathrm{E_g}^{InN}$: the bandgap energy of the InN [eV].

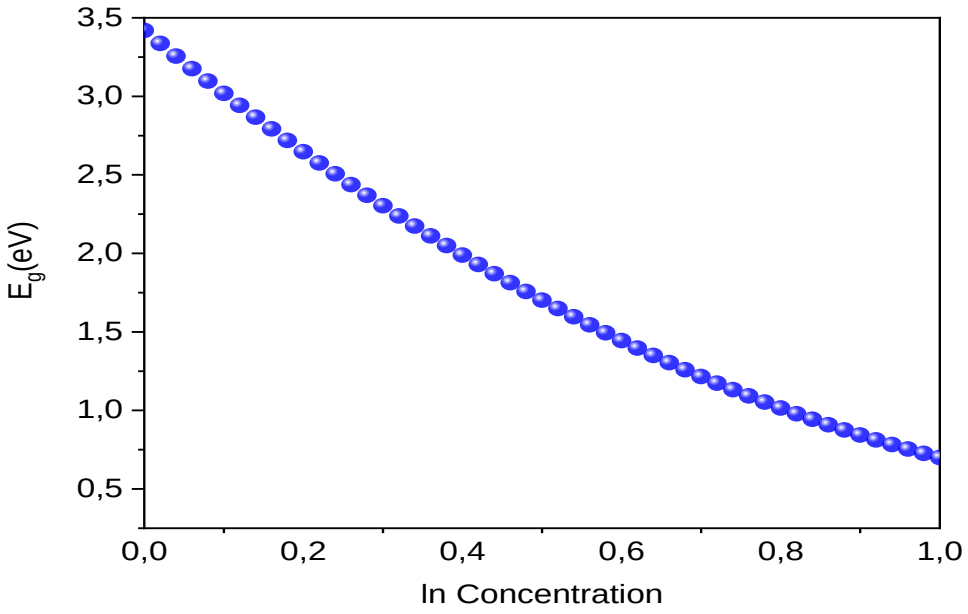

*Figure 2. 5*Evolution of the bandgap energy of the InGaN according to the concentration of Indium by introducing the curvature bowing parameter

2.4.9 The critical thickness

It is well known that during epitaxial growth, the thickness of the epitaxial layer exceeds a limit value called critical thickness (hc), the stress relaxes. When the lattice mismatch between the substrate and the epitaxial layer is weak, the first layers deposited elastically accommodate the substrate parameter and the result is the formation of a strained layer [50,51].However, if the thickness of the epitaxial layer is greater than the critical thickness, the disagreement is then overtaken by the generation of dislocations at the growth interface. These dislocations propagate from the substrate to the growth interface and the layer begins to relax. For our study, we used the most classic model, that of K. Köksal et al[52] .

$$h_c = \frac{a_e}{\sqrt{2}\Pi k\Delta}.\frac{1-0.25*\gamma}{1+\gamma}.\ln\left(\frac{h_c.\sqrt{2}}{a_e}+1\right) \qquad 1.45$$

with:

Δ : The parametric detuning which is given by:

$\Delta = \left|\frac{a_s - a_e}{a_s}\right|$ 1.46

γ: The Poisson's ratio which is given by:

$\gamma = \frac{C_{12}}{C_{11}+C_{12}}$ 1.47

- a_e: Parameter of lattice of the relaxed layer.
- k: It is a coefficient equal to 1 in the case of a super-lattice, to 2 for a quantum well ,4 in the case of a single layer.

(Refaire le graphe)

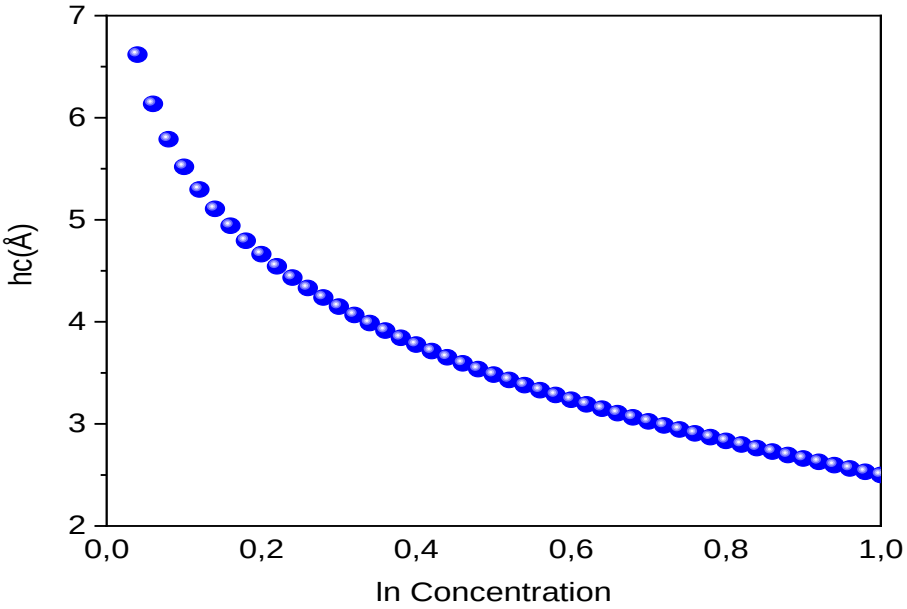

*Figure 2. 6*Shows the variation of critical thickness (hc) according to indium concentration

For the structure InGaN with GaN Layer we have traced in figure 2. 6the variation of critical thickness (h_c) as according to indium concentration. We notice that indium has the effect of reducing the critical thickness for an extensive stress.

2.4.10 Interest of lnGaN for solar cells

a. Simple *Junction*

During 2008 and 2009, several research projects were carried out on homo-junction photovoltaic cells based on InGaN, this research was specifically aimed at obtaining better experimental yields. Due to the fact that the latter did not correspond to the theoretical Efficency because of several factors such as the complexity of introducing indium with GaN, the very high concentration of electrons in the GaN or the formation of an ohmic contact between the GaN p-type and metal. However, research by Chen, X and Cai, 1. M on the common voltage characteristics of an InGaN-based homojunction cell with respect to the indium concentration.

b. Heterojunctions

Other research was done by a certain Kurtz on heterojunction cells at base of the InGaN / Si alloy, the theoretical results obtained by the author have demonstrated a fairly convincing return of 39% with the respective gaps of 1.1 and 1.75 eV including the gap of lnGaN was obtained with 50% indium. This also allows to have a junction low resistance ohmic due to the overlapping of the bottom of the lnGaN conduction bandwidth the top of the Si valence band, as reported by L. Hsu and W. Walukiewicz [48,49]. In particular, studies conducted by R. Dahal in 2010 with the aim of improving the quality crystalline material, which proposed a new heterojunction cell structure Multi quantum well InGaN / GaN deposited between two layers of N and P type GaN in as active layers.

c. Multi-junctions

Multi-junction cell technology helps optimize spectrum absorption solar power and thus obtain better yields. For this, several P-N junctions, with different energy gaps, are stacked. The top cells have a gap optimized for short wavelengths in the blue (high energies). Cells of medium have a gap in the visible or near infrared. Finally, the bottom cells have an optimized gap in the middle infrared and long wavelengths (small energies). The cells are connected in series using tunnel junctions. Most often these cells are made up of three junctions, but ideally it would take a very large number of junctions in order to better capture the solar spectrum.

2.5 Conclusion

In this chapter, we have presented in details the operating principle, the electronic and optical characteristics and properties of the InGaN (large direct gap according to all compositions that can open almost the entire solar spectrum).

3.1Introduction

In this chapter, we present the study of the InGaN/GaN structure. In the first part, we define the structure to be simulated as well as the parameters used. These parameters are chosen according to the technological means used in the production of the photovoltaic cells. We then present a description of the simulation software of the company SILVACO and its implementation within the framework of our work.

In a second part, we describe a two-dimensional simulation study carried out under SILVACO / ATLAS and we present the results obtained from the numerical simulation of the structure with inter-digitized rear contacts. In addition, the results of the simulation made it possible to study various parameters influencing the performance of cells.

3.2 Introduction to Silvaco TCAD

In this thesis research, Silvaco TCAD Software is chosen as simulator to build the models of solar cell and to simulate.

Silvaco TCAD (Technology Computer Aided Design) is a powerful device design and simulation software, including both semiconductor process simulation and device simulation. This software is developed by SILVACO, Inc.

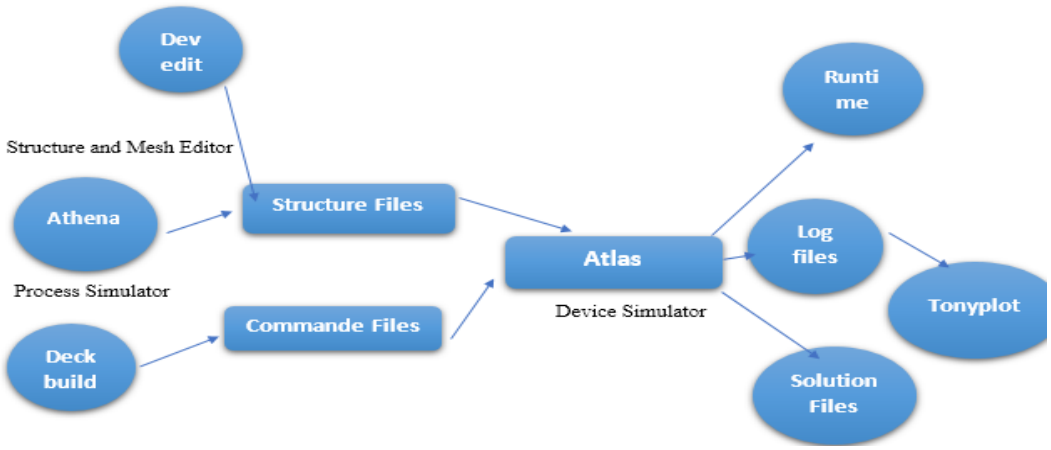

Figure 3. 1: Simulation flow diagram of Silvaco TCAD [55]

As shown in Fig. 3.1, Silvaco TCAD contains many different parts, such as interactive tools DeckBuild and Tonyplot, process simulator ATHENA, device simulator ATLAS, structure and lattice editor DevEdit, and so on. Fig. 3.1 describes the flow diagram when simulating through Silvaco TCAD. All these parts are organized together through DeckBuild interface.

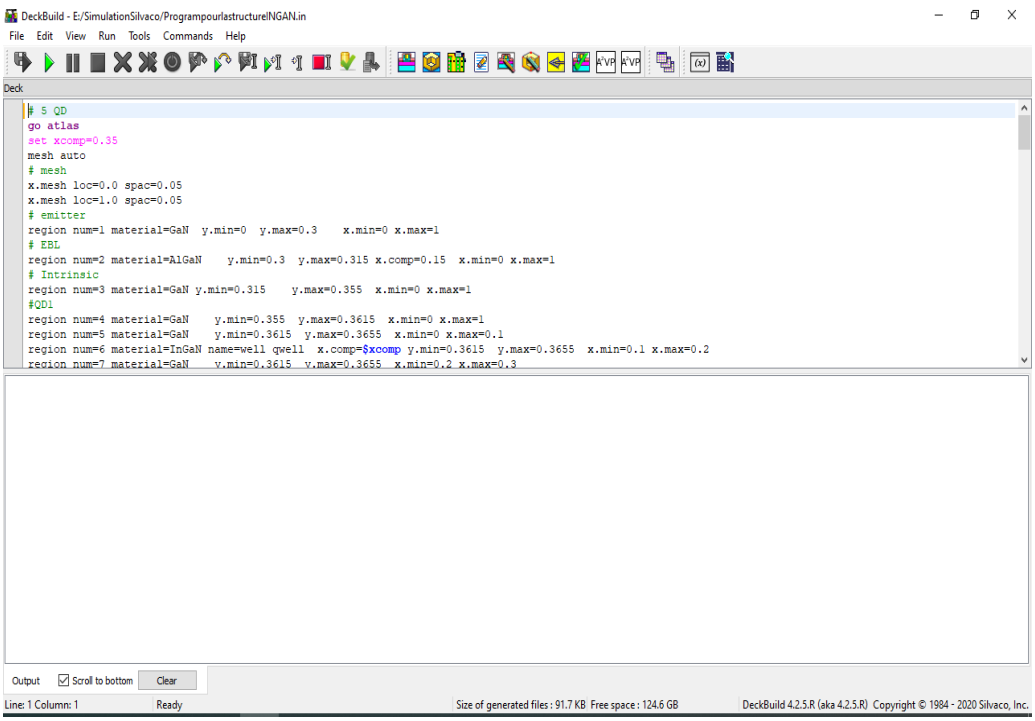

Figure 3. 2 : Interactive tool Deck Build [56]

Fig. 3.2 shows the graphical user interface of Silvaco TCAD, which is named Deck Build. In the upper window of Deck Build, user can write interface language to command certain actions and describe such as the structure of device, physical calculation model, output parameters and so on. After simulating and calculating, the results and output data will be shown in the lower window of Deck Build.

From Fig. 3.1, we can see that device simulator ATLAS is the core part of Silvaco TCAD software. It can simulate many characteristics of a semiconductor device completely, including electrical behavior, optical behavior, thermal behavior, and so on. ATLAS provides an easy-to-use, modular and extensibleplatform, which is based on physics. In addition, ATLAS affords a large number of physical calculation models for users to choose.

As a device simulator, ATLAS owns a full set of functions from building models to

calculating out results. All these functions are achievedthrough statement description. ATLAS statements can be classified into different groups by five different functions, which are structure specification, material models specification, numerical method selection, solution specification, results analysis, respectively.

the primary statements in each ATLAS command groups are:

1) Structure specification: Including the division of lattice, definition of regions with different materials, definition of electrodes, and setup of doping concentration.

2) Material models specification: Including setup of material parameters (band gap, absorption coefficient, minority lifetime, electron affinity etc.), choose of physical models, specification of contact characteristics, and definition of interface properties.

3) Numerical method selection: Computer simulation is based on numerical calculation. To make sure that the calculation can converge, numerical method should be selected properly. In ATLAS, there are Newton iteration method, Gummel iteration method, Block iteration method, and combination iterationmethod.

4) Solution specification: Obtain device working characteristics by setting up voltages, currents, illumination, and so on.

5) Results analysis: To help analyze, specified data or values can be extracted from simulation results obtained in previous steps. Figures and curves can also be extracted and plotted through simulation results.[55,56].

3.3Structure of the standard PV cell

The key structure of a GaN solar cell is a PN junction, as shown in Figure 3.3. Then, other layers are deposited around the PN junction, such as the window layer, the anti-reflective layer, the rear surface layer, and metal electrodes.

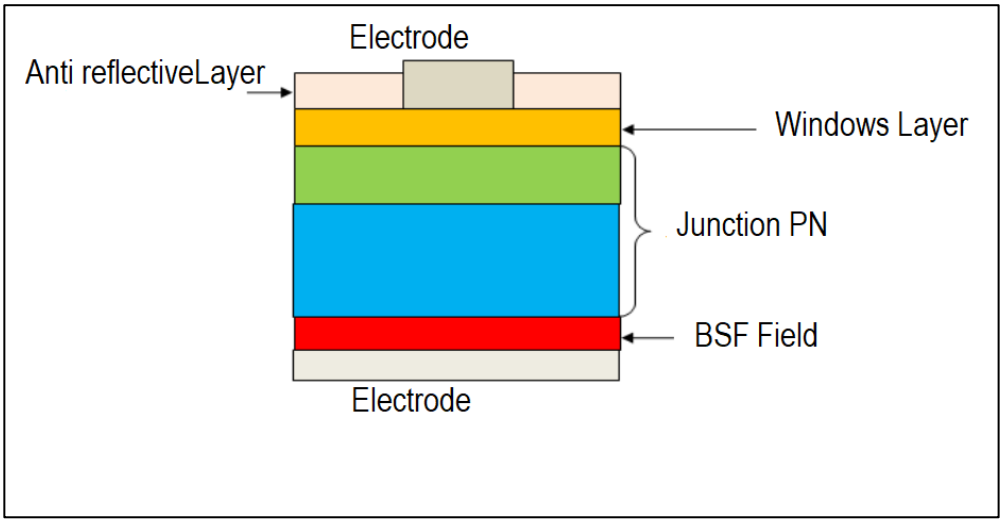

Figure 3.3 structure of InGaN/GaN PV cell [54]

The PN junction is used to set up the high electric field and space charging area, which are the key factors to help photo-generated carriers get away and generate electricity. Photons spread exponentially in semiconductors. In addition, most photo-generated carriers, which are useful for the photon current located at the diffusion region and drift region. Thus, the PN junction should be close to the upper surface of the solar cell. Therefore, the PN junction structure is generally designed to have a thicker, thinner lower top layer, as shown in Figure 3.3. In addition, since the mobility of the holes is significantly lower than the mobility of the electrons, the thinner upper part is generally carried out in the p-type form and the thicker lower lateral region is generally carried out under the n-type region. As a result, holes with low mobility will have shorter drift distance, and high-mobility electrons will drift further away.

The window layer is mainly used to reduce front surface recombination. For materials that can be chosen as a window layer, there are several requirements. First, it should have better transmission, and most of the light should not be absorbed by this layer. Thus, semiconductor materials with a high band interval can be used as a window layer. In addition, the layer must be very thin to reduce the absorption of light. On the other hand, for good contact with metal electrode, the concentration of the window layer must be higher than the concentration of type p regions. Figure 3.3 is the energy band diagram of the p-type window layer, which can help explain the positive effect of the window layer.

3.4Structure of the p-i-n photovoltaic cell

Our goal in this thesis is to build the model of simulations using Silvaco TCAD for solar cells and try to compare the simulations with actual measurement data. Thus, we used the data and measurement in Dr. Bailey's research [37].The solar cell structure comes from an actual solar cell chip [37], which contains measurement data from experiments. The Structure we built to simulate that in measure [37].

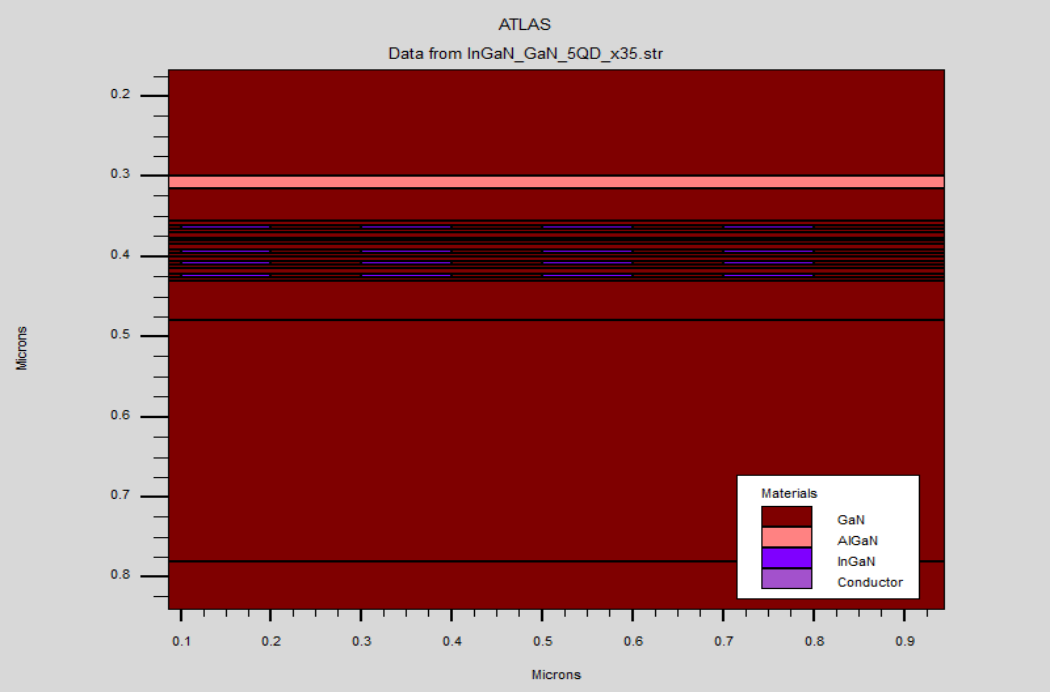

Figure 3. 4: Structure of InGaN / GaN of quantum dots with 5 layers created in the intrinsic region

doped region:

This figure here shows the different concentration in different regions of our Quantum dot structure used in this research:

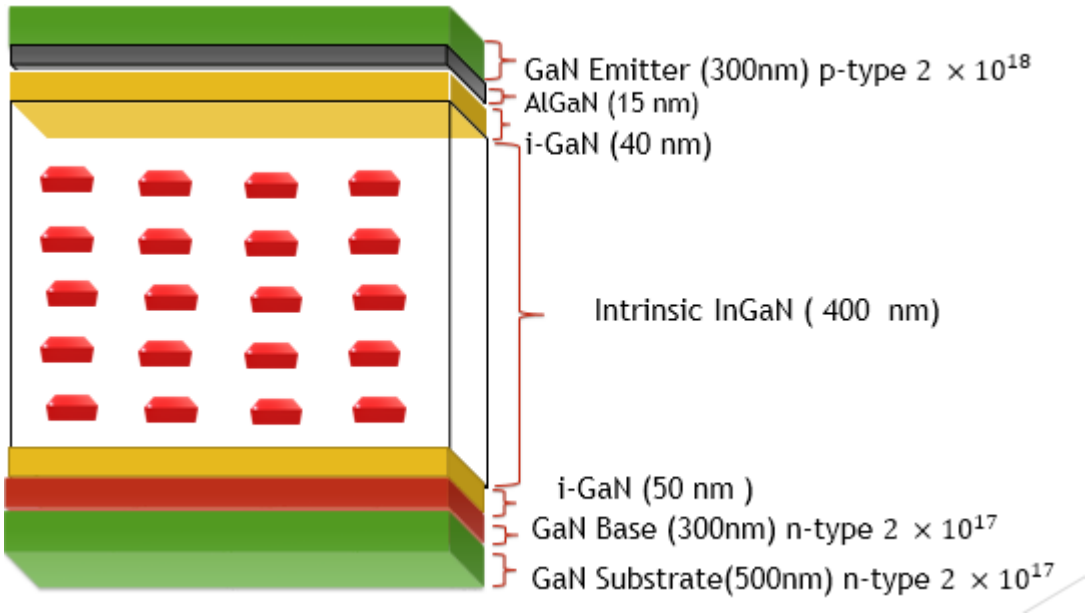

3.5 The simulation results the p-i-n photovoltaic cell

The Table shows the simulation results of the p-i-n photovoltaic cell, which contains J_{sc} short-circuit current, V_{oc} open-circuit voltage, FF fill factor, and conversion efficiency. They are the most important parameters for defining photovoltaic cells. And we're going to compare these results with the results of a quantum dots inserted.

x=15%	J_{sc} (mA/cm²)	V_{oc} (V)	FF (%)	η (%)
P-i-N , no QDs	9,96	1,6589	74,17	12,26

Table 3. 1: Simulation results of a photovoltaic cell After simulating the structure of a p-i-n no QDSC

3.5.1 Simulation results for different Indium concentration:

In this section, the results of the simulation of the photovoltaic cell inserted by quantum dots of InGaN/GaN will be presented. First, all the settings important solar cells, such as the short-circuit current, the circuit voltage open, the fill factor and the conversion efficiency, are compared between the measurement data of the quantum dots structure and the results of the simulations shown below. Table 1 shows the simulation results of photovoltaic cells for different x, for x = 15%, x = 25% and x = 35% under room temperature (300K) . We notice that each time to increase 'x' the parameters of the cell changes, and we find that the optimal value is when x= 15%.

5QDs	J_{sc} (mA/cm²)	V_{oc}(V)	FF (%)	η (%)
P-i-N , no QD	9,96	1,66	74,17	12,26
x= 15%	14,99	1,35	65,19	13.18
x = 25 %	14,55	1,30	62,11	11,72
x = 35 %	14,26	1,28	60,38	11.03

Table 3. 2 Electrical characteristics of p-i-n solar cell and QDSC for 5 QD layers.

Fig 3.5 shows the curves of Photovoltaic cell I(V) to 5 quantum dots, which are traced from the simulation results. We notice that the short-circuit current thus the open

circuit voltage increases. Then the curve of x=15% is the optimal compared to x=25% and x=35%.

Concentration of indium increases causes a decrease in short circuit I_{sc} current and efficiency.

Due to the carriers recombination electrons/holes pairs which made a decrease of the absorption coefficient.

Also, the increase in the strain effect the stability of our structure that is why we have respecting this criterion in addition, a high efficiency and high $J_{SC}$are obtained under optimum concentration values as shown in Fig. 3.5

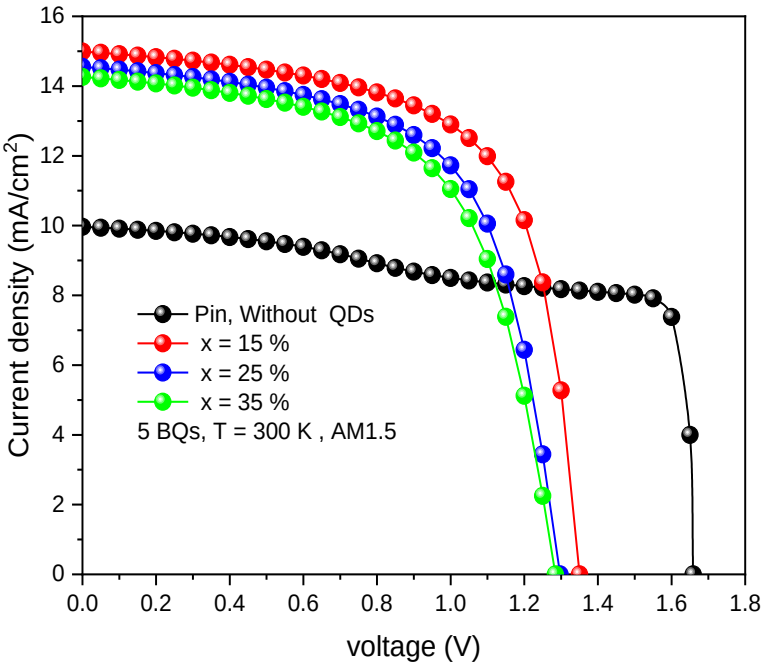

*Figure 3. 5*J-V Characteristics of the InGaN/GaN QDSC for 5 QD layers inserted and for a variable indium concentration (x=15, 25 and 35%)

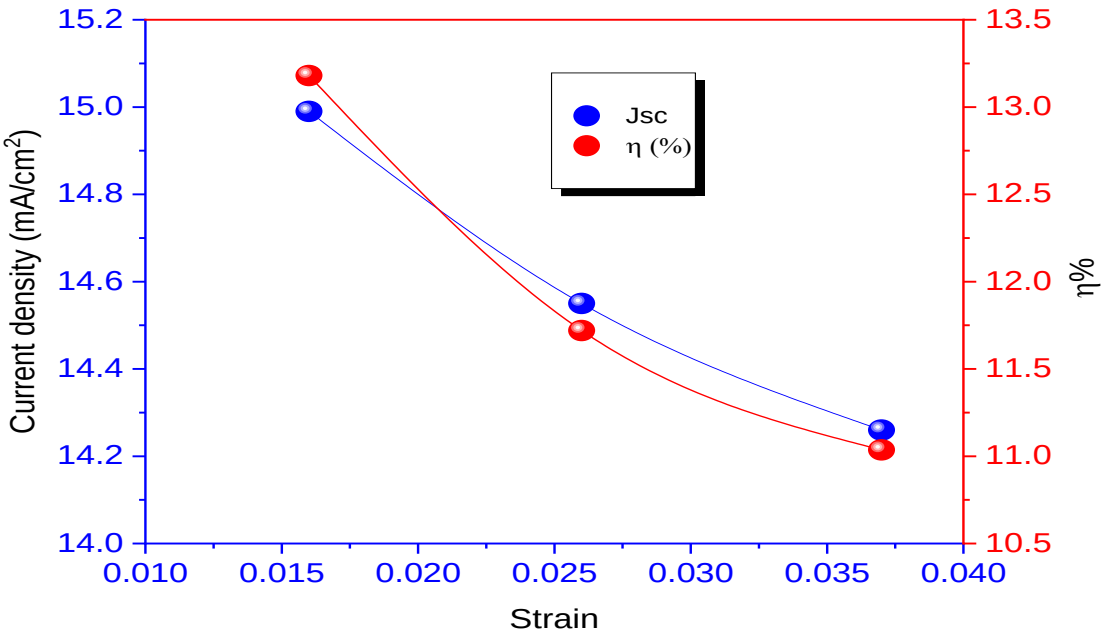

*Figure 3. 6*Variation of efficiency and short current density according to the strain

3.5.2 Simulation results for 5, 10, and 15 Quantum dots:

Effect of inserting quantum dots on I (V):The following table shows the parameters of 3 quantum dots structures:

x=15%	Jsc (mA/cm^2)	Voc (V)	FF (%)	η (%)
PiN , no QD	9,96	1,66	74,17	12,26
5 BQs	14,99	1.35	65.19	13.18
10 BQs	11,52	1.332	62.52	9.59
15 BQs	7,19	1.32	58.26	7.187

Table 3. 3 *Electrical characteristics of p-i-n solar cell and QDSC for fixed concentration (x=15%).*

Table shows the simulation results for different quantum dots inserted in a p-i-n., which are 5-layers, 10-layers and 15-layers, respectively:

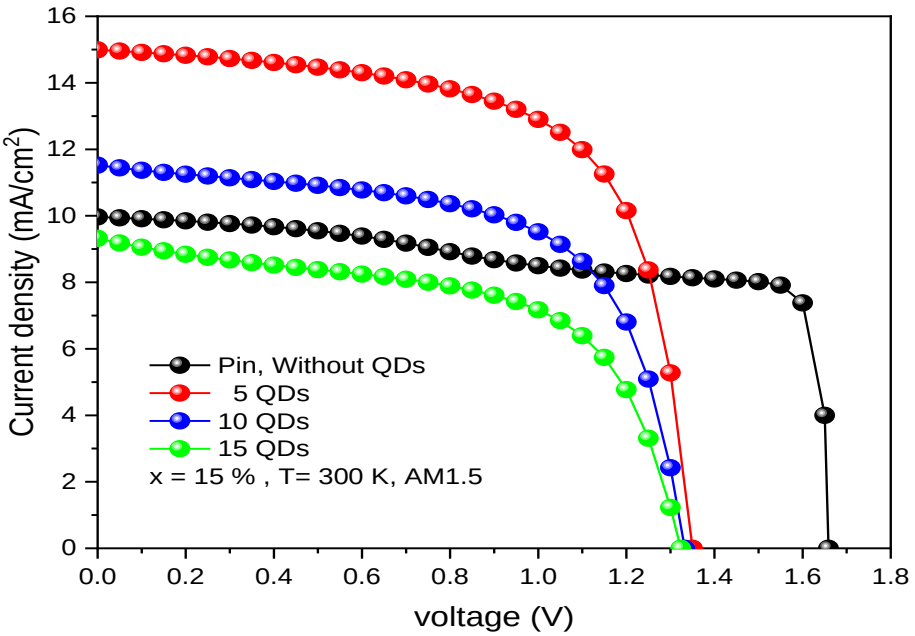

Figure 3. 7 J-V Characteristics of the InGaN/GaN QDSC for different layers inserted and for a variable fixed concentration(x=15%)

Figure 3.7 represents the current-voltage J-V characteristics of InGaN/GaN QDSC for a variable number of quantum dot layers inserted: 5, 10, 15respectively. Table includes all the characteristics parameters of the solar cell achieved in our simulation for a different number of quantum dots. As can be seen, the I_{sc} increase when the number of QD layers decreased. This enhancement in the short circuit current is due to the absorption of the photons with lower energy, which means more electron-hole pairs photo generated. Also, the open circuit voltage almost stays the same. As a result, the conversion efficiency increases from 12.26%

to 13.18 % when comparing 5QDs inserted with standard Pin noQDs.

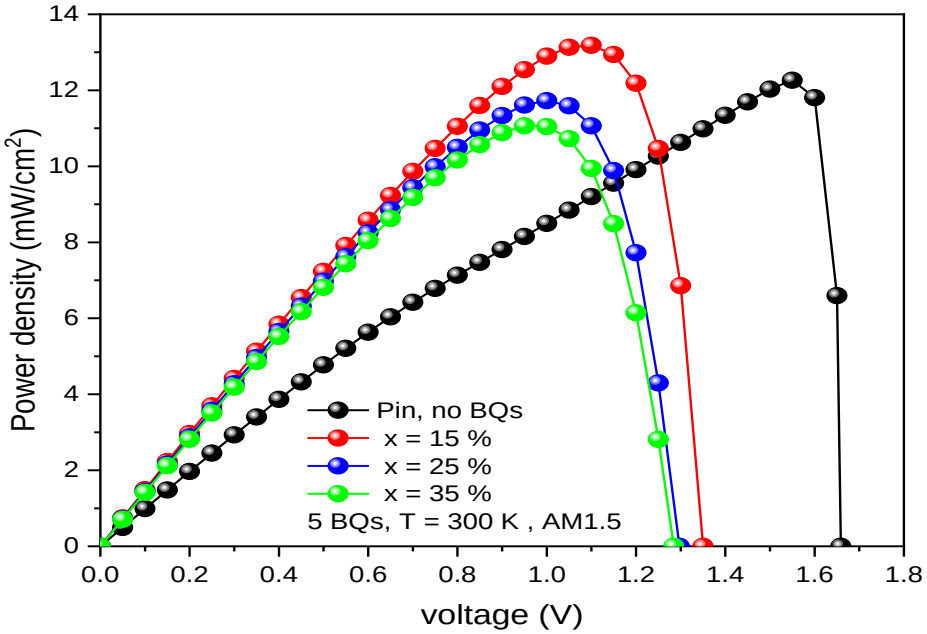

Figure 3. 8 P-V Characteristics of the InGaN/GaN QDSC for 5 QD's layers inserted and for a variable indium concentration (x=15, 25 and 35%)

As can be seen, the power freed by this structure increase when the number of QD layers 5 Quantum dots. This is due to the enhancement of the short circuit current. This enhancement in the short circuit current is due to the absorption of the photons with lower energy, which means more electron-hole pairs photo generated.

Figure 3.9 represents the current-voltage J-V and the power-voltage P-V characteristics of InGaN/GaN QDSC for a variable Indium concentration (x): 15,25, and 35% respectively.

As can be seen, the power freed by this structure increase when the concentration is x= 15% percent. This is due to the enhancement of the short circuit current. This enhancement in the short circuit current is due to the absorption of the photons with lower energy, which means more electron-hole pairs photo generated.

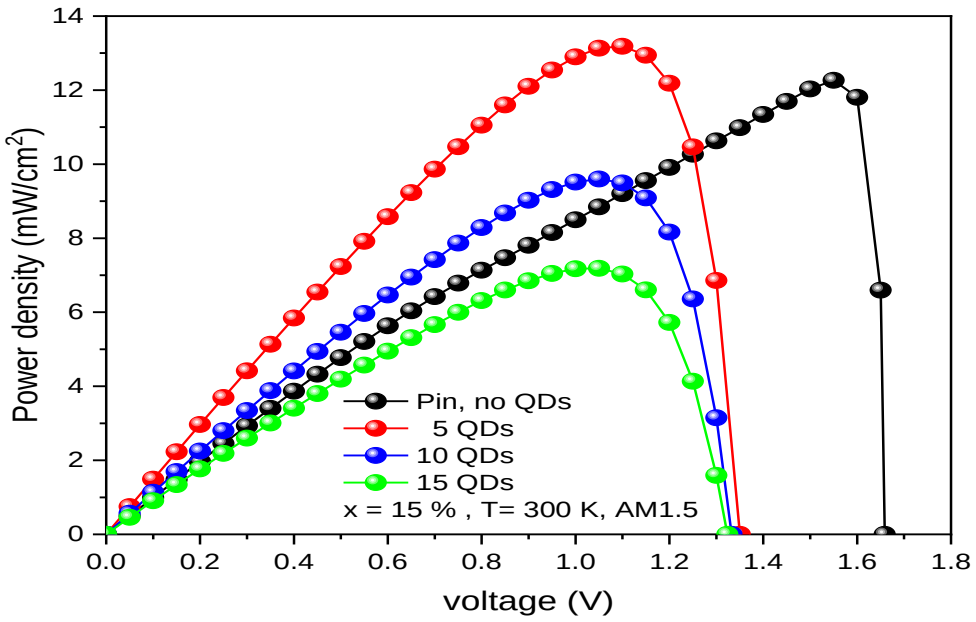

Figure 3. 9 P-V Characteristics of the InGaN/GaN QDSC for different layers inserted and for a variable fixed concentration(x=15%)

Figure 3.9 represents the current-voltage J-V and the power-voltage P-V characteristics of InGaN/GaN QDSC for a variable number of quantum dot layers inserted: 5, 10, and 15 respectively.

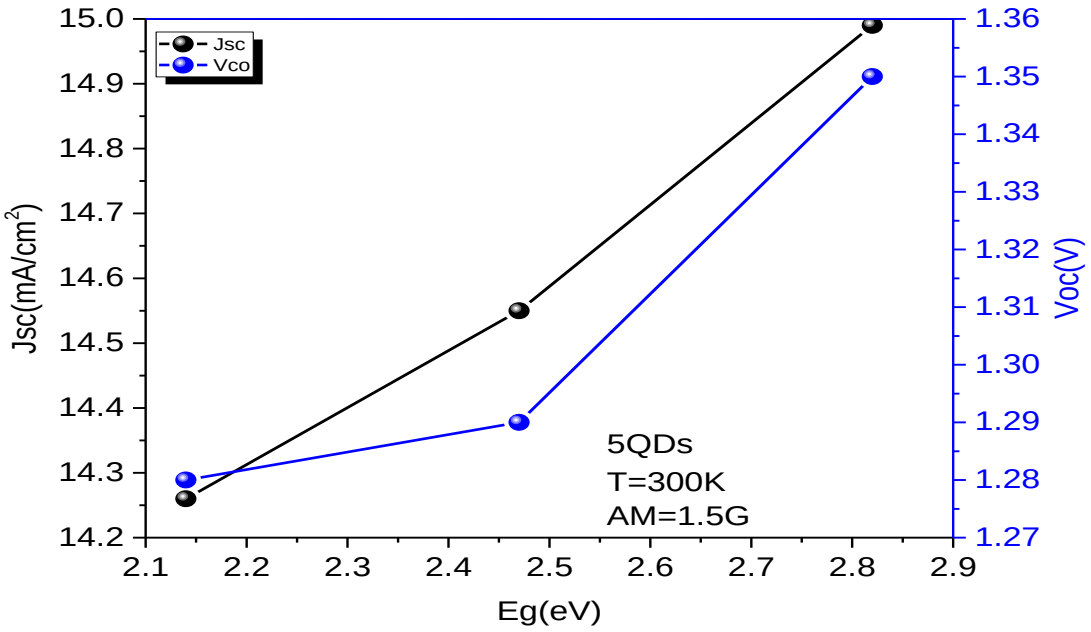

Figure 3. 10:Variation de I_{sc} et Voc en fonction de E_g

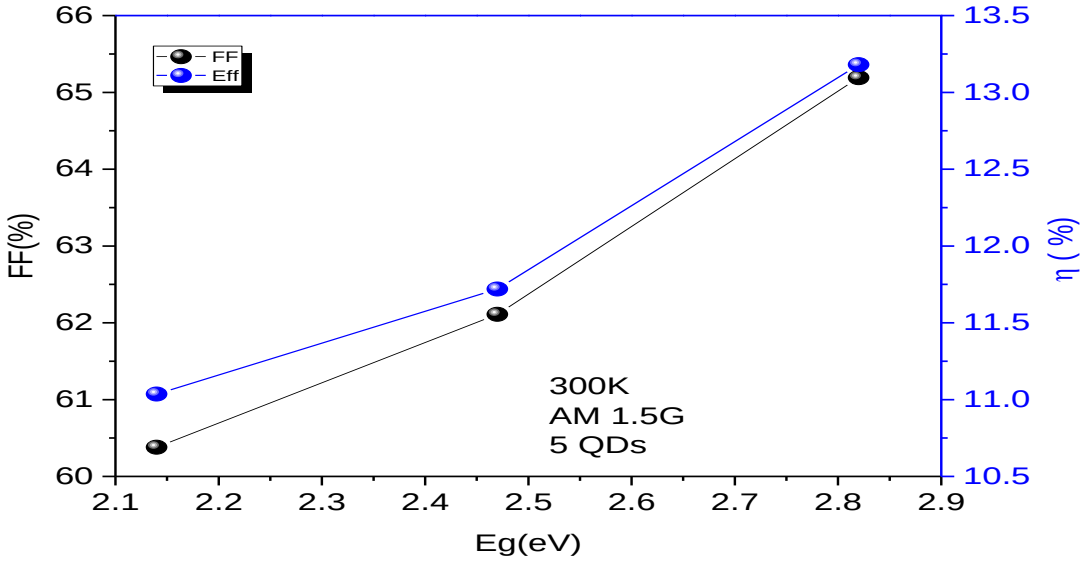

Figure 3. 11 Variation of fill factor and efficiency according to Eg

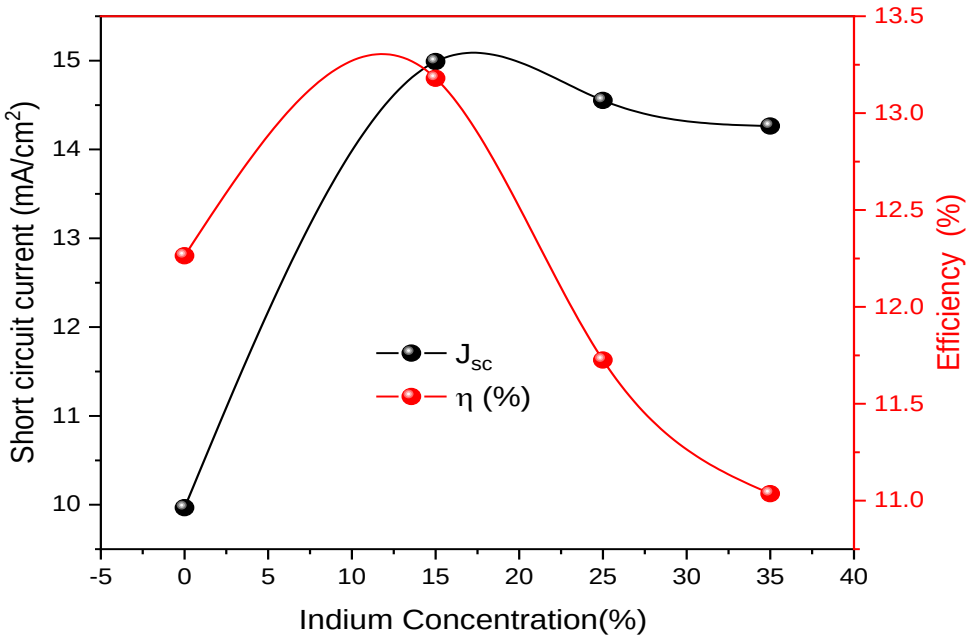

*Figure 3. 12*Variation of short-circuit density current and efficiency as function of Indium fraction

Fig 3.12represents both the variation of short-circuit density current J_{sc} and efficiency as function of the Indium mole fraction in the In(x)Ga(1-x)N/GaN ranging from x=0 to x=35%.As we can see, the short circuit density current is increasing with incontent. Increasing the x fraction of the indium in the InGaN/GaN quantum dots leads to raise the strain effect and therefore the increasing the recombination of the carriers and that reduce also Energy band gap in such structures.It's clear that the indium fraction x=15% gives the maximum efficiency of about 13.2%.

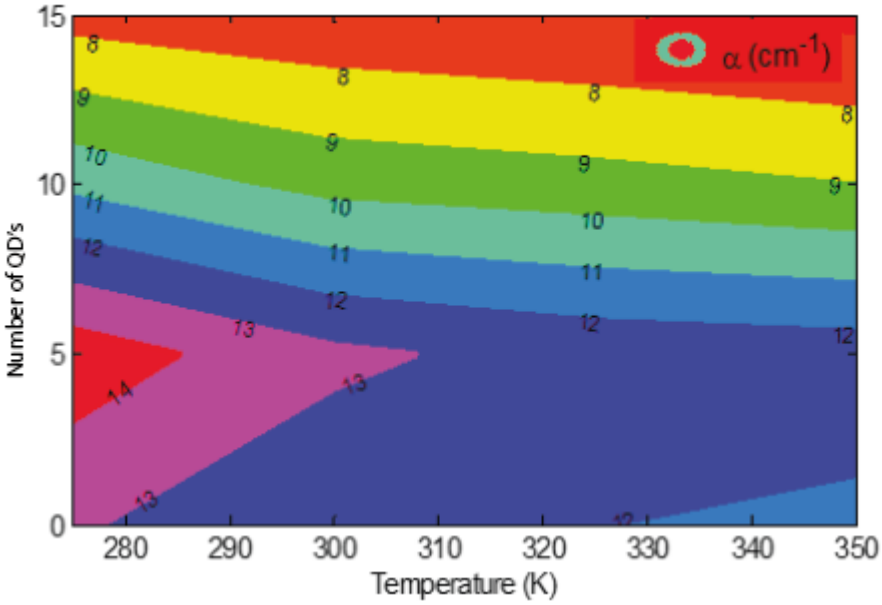

Figure 3. 13: Variation of efficiency as a function and QDs numbers

Fig 3.13. illustrate the variation of efficiency as function of temperature and QDs number. We note that on the one hand the efficiency decreases when the quantum dots increase. On the other hand it is obvious that the efficiency decreases when the temperature increase For example for 5 layers of InGaN/GaN inserted in the intrinsic region and for the temperature 275 K we have an open circuit voltage of 1.38 V and when the temperature increases to a value of 350 K the open circuit decrease to 1.27V. as result the conversion efficiency decreases from 14.58 % to 12.44% . We can explain this decrease by the reducing in the band gap of solar cell, which has an effect in the decrease of open circuit voltage.So, the temperature dependences of the short circuit current, open circuit voltage and conversion efficiency of InGaN/GaN QDSC are calculated and shown in Table below.

Conclusion

In this chapter, we have simulated in details variouscharacteristics of inserting different layers 5,10 and15 Quantum dots respectively and for three different concentration x=15 , 25 and 35% respectively , We conclude that x = 15 % and the 5 QDs have the optimal results increasing the efficiency to 13.18%.

General Conclusion

As part of this work we have studied the structure of a photovoltaic cell based on InGaN/GaN. In the 1 chapter we spoke in a general wayabout the photovoltaic effect which consists in defining the semiconductors, the effects, the basic elements forming a photovoltaic cell ... etc.In chapter2 we described quantum dots and presented the various optical and electronic parameters of the alloy (InGaN/GaN).

InGaN is a semiconductor material made of a mix of gallium nitride (GaN) and indium nitride (InN). It is a ternary III-V direct bandgap semiconductor. Its bandgap can be tuned by varying the amount of indium in the alloy. In(x)Ga(1 – x)N has a direct bandgap span from the infrared (0.69 eV) for InN to the ultraviolet (3.4 eV) of GaN.

We performed an extensive simulation study for aInGaN/GaN quantum dots solar cell usingSilvaco Atlas. After programming and building complete data library of material parameters, models with different parameters are built and simulated. We achieved a several results as shown below. The insertion of 5-layersofIn (0.25)Ga(0.75)N/GaNQDs inside i-region of p-i-n GaN enhances relatively the conversion efficiency. Indium fraction x=15 % gives maximum efficiency of about 13.18%.

We can conclude that the experimental part of this study in laboratory in the future can support our theorical results positively and that the solar cell based on InGaN can work with good performance.

T=275 K				
x=15%	pin	5 QDs	10 QDs	15 QDs
Jsc (mA/cm2)	9,94	14,78	11,23	8,85
Voc (I)	1,66	1,387	1,37	1,36
FF (%)	79,31	71,08	69,11	62,52
η (%)	13,09	14,58	10,70	7,53
T=300 K				
x=15%	pin	5 QDs	10 QDs	15 QDs
Jsc (mA/cm2)	9,96	14,99	11,52	7,18
Voc (I)	1,65	1,35	1,33	1,32
FF (%)	74,17	65,19	62,52	58,26
η (%)	12,26	13,18	9,59	7,18
T=325 K				
x=15%	pin	5 QDs	10 QDs	15 QDs
Jsc (mA/cm2)	10,04	14,77	11,48	9,49
Voc (I)	1,65	1,31	1,30	1,29
FF (%)	73,80	70,23	62,21	56,71
η (%)	12,01	12,62	9,31	6,96
T=350 K				
x=15%	pin	5 QDs	10 QDs	15 QDs
Jsc (mA/cm2)	10,27	14,97	11,54	10,01
Voc (I)	1,65	1,27	1,26	1,25
FF (%)	69,51	65,04	61,44	53,01
η (%)	**11,82**	**12,44**	**8.98**	**6,68**

*Table 3. 4*Electrical characteristic of p-i-n solar cell and QDSC for different temperature extracted from Silvaco

References

[1] P.M. Petroff, A. Lorke, A. Imamoglu, Epitaxially self-assembled quantum dots, Phys.Today 54 (5) (2001) 46–52.

[2] D. Pan, Y.P. Zeng, M.Y. Kong, New method for the growth of highly uniformquantum dots, Microelectron. Eng. 43–44 (1998) 79–83.

[3] S. Maimon, E. Finkman, G. Bahir, S.E. Schacham, J.M. Garcia, P.M. Petroff,Intersublevel transitions in InAs/GaAs quantum dots infrared photodetectors, Appl.Phys. Lett. 73 (14) (1998), 2003–5.

[4] Tahanout, C., ''Etude, simulation électrothermique d'un Micro Capteur de gaz àbase d'oxyde semi-conducteur'', Université M'hamedBougara-Boumerdes, (2010).

[5] Rahal, F., ''Etude comparative des couche minces de Ti à la conception desCellulesphotovoltaique obtenues par différentes méthodes'', Université de M'sila,(2009).

[6] Hamada, H., ''circuits électroniques'', OPU, (1993)

[7] Benahmed, N., '' Propriétés physiques des semi-conducteurs (Si monocristallin etGe) et Simulation des cellules solaires à base de Si et SiGe'', Université AboubakrBlkaid-Telemcen, (2006).

[8] Mathieu, H.,''Physique des semi-conducteurs et des composants électroniques'',Masson, Paris, (1996).

[9] I. Sari-Ali, B. Benyoucef, B. Chikh-Bled., ''Etude de la jonction PN d'un semi-conducteur à l'équilibre thermodynamique'', Journal of Electron Devices, Vol. 5, pp.122-126,(2007).

[10] AkassewaTchapo , S., ''Système d'alimentation photovoltaïque avec stockagehybride pour l'habitat énergétiquement autonome'', Université Henri Poincaré,NancyI, (2010).

[11]Benmachiche, S., '' Etude des paramètres limitant le rendement d'une photopile àbase d'une structure MIS'', Université Hadj Lakhdar-Batna, (2009).

[12] Thibaut, D., ''Développement de cellules photovoltaïques à hétérojonctionssilicium et contacts en face arrière'', Institut National des Sciences Appliquées deLyon,(2009).

[13] Madani, M., ‘’Réalisation des couches antireflets dans les cellules solaires àcouches minces’’, Université AboubakrBlkaid-Telemcen, (2006).

[14]Oleksiy, N., ‘’ simulation,Fabrication et analyse de cellules photovoltaïques àcontacts arriérés interagîtes ‘’, Institut national des science appliqués de Lyon, (2005).

[15] Lakehal, B., ‘’ Etude des propriétés électriques d’une photopile à base d’unestructure Schottky’’, Université de Batna, (2009).

[16] Soga, T., ‘’Nanostructured Materials for Solar Energy Conversion’’, Elsevier,Nagoya, Japan, (First Edition 2006).

[17] +hamaguchi, c., ‘’Basic Semiconductor Physics’’, Springer Heidelberg DordrechtLondon New York, (Second Edition 2010).

[18] Lelievre, J.-F., ‘’Elaboration de SiNx:H par PECVD: Optemisation des PropriétésOptiques, Passivantes et Structurales pour Applications Photovoltaïques’’, InstitutNational des Sciences Appliquées de Lyon, (2007).

[19] Abdo, F., ‘’Croissance des Couches minces de Silicium par Epitaxie en PhaseLiquide à basse Température pour Applications Photovoltaïques’’, Institut Nationaldes Science Appliquées de Lyon, (2007).

[20] Damon-Lacoste, J.,’’Vers une Ingénierie de Bandes des Cellules Solaires àHétérojonctionsa-SI:h/c-SI.RôlePrépondérantdel'Hydrogène’’,EcolePolytechnique,Paris, (2007).

[21]Silvestre,I. C., ‘’Modelling Photovoltaic Systems Using Pspice’’ UniversidadPolitecnica de Catalunia, barcelona, john wiley& sons, ltd,spain, (2002).

[22] L. Liu and J. H. Edgar, "Substrates for gallium nitride epitaxy", Materials Science andEngineering: R: Reports, vol. 37, pp. 61-127, 2002.

[23] Bernardini, F., Fiorentini, V. and Vanderbilt, D. ‘’Spontaneouspolarizationandpiezoelectric’’, Communications. 11, 1972, 617.

[24] Thibaut DESRUES, ‘’Développement de cellules photovoltaïques à hétérojonctionssilicium et contacts en face arrière ‘’, Thèse de Doctorat, L’Institut National desSciences Appliquées de Lyon, 30/11/2009

[25] J. Wu, "When group-III nitrides go infrared: New properties and perspectives",Journal of AppliedPhysics, vol. 106, p. 011101, 2009.

[26] L. Bouzaı¨ene , L. Sfaxi , M. Baira ,H. Maaref , and C. Bru-Chevallier «Power density and temperature dependent multi-excited states in InAs/GaAs quantum dots»,

[27] R. Krahne, G. Morello, A. Figuerola, C. George et S. Deka, and M. Liberato« Physical properties of elongated inorganic nanoparticles,»Physics Reports, 50175-221, (2011).

[28] A.P. Alivisatos, « Semiconductor clusters, Nanocrystals, and quantum dots.,» Science 271. , n° 116 February(1996).

[29] S.L. Chang, “Physics of optoelectronic devices”, N.Y. Wiley(1995).

[30] EL GMILI Youssef, ‘’Etude et caractérisations par cathodo-luminescence de couchesminces d’InGaN pour le photovoltaïque’’, Thèse de doctorat. L’UniversitédeLorraine&l’Université Sidi Mohamed Ben Abdellah–Fes, 2013**”.**scanningtransmissionelectron microscopy’’, Nature Materials, 2009, Vol. 8, p. 263

[31] H. P. Rocksby, «Thecolour of seleniumrubyglasses,,» J. Soc. Glass. Techn,16,. 171-181(1932).

[32] Y. Arakawa and H. Sakaki, « Multidimensional quantum well laser and temperature dependence of its threshold current,» Appl. Phys. Lett. 40, 939,1982).

[33] D.Bimberg*et al* «Quantum Dot Heterostructures »Wiley, Chichester,1998.

[34] D. Pan, E. Towe and S. Kennerly, "Tuning of conduction intersublevel absorption ... quantum dot infrared photodetectors," Electron Lett. 34, 1883(1998).

[35] K. Imamura, Y. Sugiyama, Y. Nakata, S. Muto, and N. Yokoyama, Jpn. J. Appl. Phys., Part 2 34, L1445(1995).

[36] C.H. Bennett, G. Brassard, C. Crépeau, R. Jozsa, A. Peres, and W. K.Wootters«Teleporting an unknown quantum state via dual classical and Einstein Podolsky- Rosen channels,» Phys. Rev. Lett. 70, 1895 – 1899 (1993).

[37] CS.M. Hubbard, C.D. Cress, C.G. Bailey, S.G.Bailey, D.M. Wilt, and R.P.Raffaelle Appl. Phys. Lett. 92, 123512 (2008).

[38] A. Marti, E. Antolin, C. R. Stanley, C. D. Farmer, N. Lopez, P. Diaz, E. Canovas,P.G. Linares, and A. Luque Phys. Rev. Lett. 97, 247701 (2006).

[39]N. N. Ledentsov, Semicond, Sci. Technol. 26, (2011)014001.

[40]P.Michler,« Single quantum dots » Springer,2003.

[41]A. Scherer, and H.G. Craighead, Appl. Phys. Lett., 49 1284 (1986).

[42]M. Volmer, Z. Phys. Chim. 119,277(1926).

[43]JanH.Van Der Merwe and E. Bauer, Physical Review B, 39 3632(1989).M. Bayer *at al*, "Hidden symmetries in the energy levels of excitonic 'artificial atoms' " Nature 405, 923 (2000).

[44]Ni Chauvin. « Spectroscopie de la boîte quantique unique dans les systèmes InAs sur InP et InAs sur GaAs émettant à 1.3 µm et 1.5 µm : application aux sources localisées. » Thèse de Doctorat, Institut National des Sciences Appliquées de Lyon,(2006).

[45]Charles Cornet « Propriétés électroniques, optiques et dynamiques de boites quantiques auto-organisées et couplées sur substrat InP», thèse devant l'Institut National des Sciences Appliquées de Rennes (22 févr. 2007)**.**

[46]Yam, F.K. and Hassan, Z. InGaN, ''An overview of the growth kinetics, physicalproperties and emission mechanisms, Super-lattices and Microstructures'', 2008, Vol.43, 1.

[47] Clàudio de Carvalho, L., Schleife, A. and Bechstedt, F. ''Influence of exchange andcorrelation on structural and electronic properties of AlN, GaN, and InNpolytypes','Physical Review B. 2011, Vol. 84, 195105.''

[48]Vegard, L. Z. Phys. 1921, Vol. 5, 17.

[49] M. A. Cusack, P. R. Briddon, and M. Jaros "Absorption spectra and optical transitions in InAs/GaAs self-assembled quantum dots", Phys. Rev. B 56, 4047(1997).

[50] V. Gorge. «Caractérisations de matériaux et tests de composants descellulessolaires à base des nitrures des éléments III-V», thèse de doctorat université paris sud 11, 2012.

[51]A. AISSAT : « Modélisation et Simulation du gain optique et du courantdeSeuil d'un laser à puits quantique contraint à base de $Ga_{\chi}In_{1-\chi}N_{\Upsilon}As_{1-\Upsilon}/GaAs$»,Thèse de doctorat, Ecole Nationale Polytechnique, 2007.

[52] K. Köksal, B. Gönül, and M. Oduncuoğlu: «Critical Layer Thickness ofGaIn(N)As(Sb).

[53] A. BENAMAROUCHE Etude et simulation d'une structure photovoltaïque à basedesemiconducteurs II-VI (CdZnTe), 2012.

[54] A.BENHAMED étude et modélisation des structures a base des boites quantiques pour la conversion photovoltaïque 2017.

[55,56] SILVACO International. "NMOS Device Simulation Using ATLAS,"TCAD workshop,69-136